ECOLE POLYTECHNIQUE DE BRUXELLES

ULB

UNIVERSITÉ LIBRE DE BRUXELLES, UNIVERSITÉ D'EUROPE

Materials Selection, Sizing and Construction of an Extraction Unit for Essential Oils Using Steam Distillation and Solar Energy

Thesis presented for the purpose of awarding the Degree of
Master of Science in Electromechanical Engineering, option Aeronautics

Sabrina Orban

Director
Professor Benoit Haut

Co-supervisor
Sacha Breyer

Service
TIPs

Academic year
2012-2013

Acknowledgement

First I would like to express my gratitude to my thesis director, Benoit Haut, who trusted me with this subject. I thank him for supervising my work during this entire year, and for giving me the opportunity to acquire this first and enriching experience in the domain of development cooperation. I also thank my co-supervisor, Sacha Breyer, for the time she granted me, her help and advice regarding the African adventure, and her careful reading and corrections that helped producing this final report.

I deeply thank Adama Ouedraogo, the head of the Atelier Central de Maintenance of the Université de Ouagadougou, for the selfless welcome and the invaluable advice, that allowed bringing the construction of the prototype to a successful conclusion, despite of the short time frame. Special thanks go to all the members of the ACM team, and especially Aziz, Adama Sawadogo, Bertrand, Arnaud, Zorome, Romuald, Justin and Bassolé. Thank you for your efficient work, and the laughters.
In Ouagadougou, I also thank the President of the UO, who gave us an accommodation for the duration of our local stay. I thank the Professors Bathiébo and Ali, for their advice that helped us adapt to the new environment and their technical support.

I would like to acknowledge the Commission universitaire pour le Développement (CUD - Rue de Namur, 72-74, 1000 Bruxelles - `www.cud.be`) and the Conseil interuniversitaire de la Communauté française de Belgique (CIUF) for their financial intervention, which made the travel to Ouagadougou possible and therefore contributed to the success of this work.

I thank my father for reading, again and again, and for his invaluable support, that lasted from the first year of my engineering studies and all the way long. I also thank my grandparents for their loving eye.

Finally, a special thank goes to Chris, my partner over there. Thanks for fighting the sun, while enjoying everything else.

Abstract

Essential oils have great potential for use in traditional medicine treatments in developing countries. In order to fully exploit the value of essential oils, two key areas need to be investigated. Initial research explores oils of different plant varieties to benefit from curative properties, and secondly, research into highly efficient extraction units that utilize solar technologies to maximize the advantage of the Southern countries high solar potential. This work reaches the second research field, as it aims at constructing an efficient extraction unit prototype for didactic and research purpose at the Université de Ouagadougou, on the basis of the steam distillation process and using solar energy. In order to reach this goal, a materials selection of all parts of the extraction unit is first performed, focusing amongst other process constraints on the compatibility between the organic oils components and the materials. Then, a model of the thermal exchanges occurring in each subsystem of the unit is established, allowing for the sizing of the extraction prototype, on basis of the required superficial speed of steam through the plants bed provided in literature. Finally, a six weeks stay at the Université de Ouagadougou allows managing the construction of the prototype. The post-construction analysis of the unit performances gives mitigated results. Considering the available means, the achievable accuracy of the parabola profile is lower than expected, causing the global efficiency of the reflector, and the amount of heat available for water evaporation to drop far below the required values. However, the materials used for the construction will allow for a cleaner production of oils. Improving the solar reflector overall efficiency should allow for an optimal use of the extraction unit.

Keywords: extraction of essential oils, steam distillation, solar collector, solar concentrator, development cooperation

Abstract

Les huiles essentielles ont un grand potentiel d'utilisation dans les pays en développement dans le secteur de la médecine traditionnelle. Afin d'exploiter tout le potentiel des huiles essentielles, la recherche doit d'abord porter sur les propriétés curatives des huiles de différentes variétés de plantes, et ensuite, sur des techniques d'extraction hautement efficaces utilisant les technologies solaires, afin de profiter du potentiel solaire élevé des pays du Sud. Le présent travail concerne le second champ de recherche, car il vise à construire à l'Université de Ouagadougou un prototype d'unité d'extraction à but didactique et de recherche, utilisant l'entraînement à la vapeur et chauffé par énergie solaire. Pour atteindre cet objectif, une sélection des matériaux de construction de toutes les pièces de l'unité d'extraction est d'abord effectuée, en se concentrant, entre autres contraintes du procédé, sur la compatibilité entre les composants organiques des huiles et les matériaux. Ensuite, un modèle des échanges thermiques de chaque sous-système de l'unité est établi, compte tenu de la taille du prototype d'extraction, sur base de la vitesse superficielle requise pour la vapeur d'eau au travers du lit de plantes. Enfin, au cours d'un séjour de six semaines à l'Université de Ouagadougou a lieu la supervision de la construction du prototype. L'analyse post-construction de l'unité donne des résultats mitigés. Compte tenu des moyens disponibles, la précision atteignable pour le profil de la parabole est plus faible que prévu, ce qui affecte l'efficacité globale du réflecteur et fait tomber la quantité de chaleur disponible pour l'évaporation de l'eau bien en dessous de la valeur requise. Cependant, les matériaux utilisés pour la construction permettront une production plus propre des huiles. Améliorer le rendement global du réflecteur solaire devrait permettre une utilisation optimale de l'unité d'extraction dans le futur.

Mots-clés: extraction d'huiles essentielles, entraînement à la vapeur, collecteur solaire, concentrateur solaire, coopération au développement

Abstract

Etherische oliën hebben een groot potentieel voor medicinale toepassingen in ontwikkelingslanden. Om het potentieel van etherische oliën volledig te benutten, moet onderzoek gedaan worden in twee richtingen. Ten eerste moet er verder gezocht worden naar de geneeskundige eigenschappen van de oliën van verschillende plantensoorten. Ten tweede, onderzoek is nodig in verband met efficiënte extractie technieken gebaseerd op zonne-energie waarvoor zuidelijke landen een hoog potentieel hebben. Dit werk, gericht op het construeren, aan de Université de Ouagadougou, van een efficiënte, stoomdestillatie gebaseerd, zon verwarmd, didactische extractie prototype, heeft met het tweede onderzoeksveld te maken. Om dit doel te bereiken, wordt eerst een materiaal selectie van alle onderdelen van de extractie-unit gemaakt, waarbij de nadruk op de compatibiliteit tussen de organische oliën en de constructie materialen van de onderdelen wordt gezet. Daarna wordt een model van de warmtewisselingen in alle subsystemen van het toestel opgesteld. Hierdoor, en op basis van de gewenste oppervlakkige snelheid van de stoom over de planten bed, wordt de dimensionering van de extractie prototype bepaald. Tot slot, de bouw van het prototype wordt tijdens een zes weken verblijf aan de Université de Ouagadougou beheerd. De post-constructie analyse van de unit geeft gemitigeerde resultaten. Gezien de beschikbare middelen, ligt de haalbare nauwkeurigheid van de parabool profiel lager dan verwacht, waardoor de gehele efficiëntie van de reflector en de hoeveelheid warmte die wordt gegenereerd om het water te verdampen, tot onder de vereiste waarden zakt. Echter zal de keus van de bouwmaterialen zorgen voor een propere productie van olie. Het verbeteren van de zonne-reflector algemeen efficiëntie moet zorgen voor een optimaal gebruik van de extractie installatie in de toekomst.

Trefwoorden: extractie van etherische olieën, stoom destillatie, zonnecollector, zonneconcentrator, ontwikkelingssamenwerking

Contents

Chapter 1

Introduction

This work is part of the inter-university cooperation that links the Université de Ouagadougou (UO) in Burkina Faso and the Université libre de Bruxelles (ULB) in Belgium since 2009. In this chapter, the context and objectives of this cooperation are first briefly explained.
The technical aspect of this thesis focusses on the extraction process of essential oils from local plants, using steam distillation and solar energy, through the materials selection, sizing and construction of a new extraction unit for didactic use in Ouagadougou. Therefore, essential oils, their properties and socio-economical values are addressed after the cooperative context. Finally, the extraction process features are approached.

1.1 Context

1.1.1 Burkina Faso

Burkina Faso is a West African country (see figure 1.1), counting 16,97 million inhabitants for a total area of 274,200 km^2 [3], [25].
Burkina Faso is listed as a «low income» country by the World Bank, which estimates the poverty rate at 45.1%[1] in 2009 [3]. Its economy relies principally on the performance of the cotton sector [4].
Sixty different ethnic groups are listed in Burkina Faso, which is characterised by important population migrations and a great mixing between ethnic groups. The population density is highly non-uniform, allowing for zones with a population density slightly higher than the world average to exist, while other parts of the country are deserted. Nevertheless, around 80% of the population lives in rural areas [25].

The country is divided into two main zones with respect to the climate: the Sahelian North, very arid (less than 600 mm rain per year), and the Soudanian Centre and South (more than 700 mm rain per year). Two seasons alternate continuously: the long dry season from October to May and the raining season from June to September. The solar flux density is globally high, with monthly direct[2] mean values that can reach 800 W/m^2 in March [14].

[1]Percentage of the population living under the national poverty line, based on the World Bank's country poverty assessments.

[2]When entering the Earth's atmosphere, the beam of nearly parallel solar rays (called ExtraTerrestrial radiation, ETR) is separated into different components by diffusing and scattering effects. The direct solar flux density, or beam component, is then the part of the ETR that directly reaches the Earth's surface, and is measured from the earth surface on a unit surface normally oriented with respect to the sun rays, i.e. for which the measurement device receives the maximum solar radiation [28]. This terminology is used further in this work.

Figure 1.1: Map showing the localisation of Burkina Faso in West Africa

1.1.2 Development Cooperation

In several domains, Burkina Faso benefits from important resources that are unexploited or only partially exploited:

Solar energy As said before, the solar potential of the country is high, which would make the use of photovoltaic panels, solar concentrators and thermal collectors highly cost-effective. These concern numerous applications, e.g. the drying of fruits, the production of electricity, the cooking of food, the heating of water. However, solar energy is almost unexploited in Burkina Faso for several reasons. First, the initial investment of a solar installation is high, and sometimes out of reach or too risky for most of the population. Moreover, there is no state policy encouraging the investment into solar technology; no state subventions are available. Finally, although the UO offers Bachelors and Masters specialised into solar technologies - taught by the UFR/SEA (Unité de Formation et de Recherche en Sciences Exactes et Appliquées, teaching and research unit for exact and applied sciences) - since 2006, the number of qualified professionals for the sizing, installation, maintenance and repair of those technologies remains too low.

Plants potential for numerous processed applications The Soudanian region of Burkina Faso allows growing particular plants, some of which are being highly exploited by the population. For example, shea butter is used for numerous applications (food, cosmetics, health), and the products are used locally as well as exported. Also, bananas and mangoes are dried in large quantities, for local and foreign trade. On the other hand, various aromatic species containing essential oils are grown in the country, e.g. the Eucalyptus. The process of extracting the oils is still subject to several studies at the UO and worldwide, in order to better understand its mechanisms. The development and/or improvement of the specific processes using local plants for various applications is of great interest, as well as their adaptation in order to use solar energy[3].

The development of all the local resources by local actors is a key factor to the development of the country. For this purpose, the Belgian CUD (Coopération Universitaire au Développement, university development cooperation) started its four years CUI (Coopération Universitaire Institutionnelle, institutional university cooperation) program in 2008, the goal of which was to

[3]e.g.: nowadays in Burkina Faso, the fruit drying process is almost essentially performed using butane gas as thermal energy source. Example: the women cooperative in Ouagadougou, producing dried mangoes for local consumption and exportation

reinforce the teaching and research at the UO. Indeed, the professors are facing too wide groups of students to teach, a lack of young scientists turning to research as a career choice and a lack of financial means for the buying of didactic material. The long term objective of the CUI aims at increasing the number of qualified professionals in all the targeted domains, and, for the scientific side, at making progress in the mastering of local processes. In this framework of **inter-university cooperation**, exchanges between students/PhD students of the UO and the ULB started: PhD students from Burkina studying chemistry had the opportunity to carry out part of their research at the TIPs service of the ULB, while Belgian Master and PhD students of the Polytechnic School or the Faculty of Bioengineers were able to choose Master projects or thesis involving a stay at the UO. The latest are since defined according to the needs of the professors of the UFR/SEA, and consist either in the on-site construction of a prototype for didactic use or the further study of a local process (e.g. food drying, essential oils extraction) by local researchers, either in a contribution to the study of one of those processes.

As part of the inter-university cooperation projects, this Master thesis focusses on the process of extracting essential oils from a set of local plants. Therefore, the next sections introduce briefly the characterisation of essential oils and the extraction techniques.

1.2 Essential Oils

Essential oils are **organic compounds** derived from aromatic plants, and can be defined as *volatile and odorous products, generally of complex composition, obtained from botanically defined herbal raw material by accepted procedures, that do not affect the nature and composition of the products* [18].

According to Lawrencet, there are about 17,500 aromatic species on Earth. The essential oils are secreted by cells which characteristics and localisation in the plant are specific to each family of aromatic plants. The oil cells can be isolated or agglutinated, in a round, rectangular or long duct form. They can be found in leaves, flowers, bark or peel. All these characteristics play a role in the choice of the extraction technique (see section 1.3).
The chemical composition of essential oils depends on the plant considered. However, it is easily determined using gas chromatography and mass spectroscopy. Moreover, essential oils are characterised by different indicators such as their colour, odour, refraction index, viscosity, etc. [16]. The theoretical compositions of the essential oils of a panel of species are listed by the European Pharmacopoeia together with their physical indicators. This provides a reference for quality assessment.

In many cultures and civilisations worldwide, essential oils constitute an important ingredient to the treatments prescribed in the frame of **traditional medicine**. Indeed, they present antibacterial and antifungal properties and are also exploited to reinforce the immune system, helping resisting against numerous pathogens. There have been campaigns of national politics led in Burkina Faso in order to promote the use of traditional medicine, while recommending a rational use of the treatments and encouraging continuous research in the domain. Indeed, traditional medicine is part of the culture of the country and allows enhancing the value of local biological resources. Moreover, a better exploitation of traditional medicine would give access to treatments to a larger part of the population, by on the one hand allowing affordable prices compared to laboratory pharmaceuticals and on the other hand providing accessible («on site») treatments for people living in rural areas (this is the case for 80% of the population of Burkina Faso) remote from any large city. Finally, it would allow reducing the import of pharmaceuticals from the North and therefore their economic dependence at the health level.

The value of essential oils is not limited to local exploitation. Indeed, essential oils are also used in the cosmetics and perfumery industries. The large interest directed worldwide to essential oils, especially since the alternative medicines recently regained popularity in occidental cultures, provides an important market that can be exploited by developing countries, the climate of which being generally favourable to the growing of numerous aromatic plants. Nevertheless, essential oils and their extraction processes are subject to many studies, in order to improve the quality of the obtained oils and to elaborate processes that would allow increasing the quantity produced.

1.3 The Extraction Process

1.3.1 Existing Processes and Corresponding Applications

As mentioned in the previous section, the definition of essential oils prohibits the alteration of their composition by the extraction process. This is an important restriction, implying that the vapour distillation based processes are selected in most cases. Sometimes the characteristics of the plants - e.g. specific localisation of the oils (cf. citrus), high fragility of the plants (cf. jasmin flowers) - and/or the oils - e.g. if one constituent is too heavy to be carried away by vapour - require the use of other methods, such as cold pressing, effleurage, solvent extraction. However, this work focusses on the extraction of essential oils using vapour distillation, thus targeting plants for which this method is adequate.

There are several variants of the vapour distillation process:

Hydro-distillation This process consists in immersing the plants in water. Using direct heating on the mixture, the water is boiled off and carries the essential oil away. Some problems of over-heating and hydrolysis of some components of the oils arise. However, this process is the best to extract the oils from certain flowers that agglomerate when wet, therefore excluding the use of steam distillation.

Steam distillation In this case, liquid water and plants are not in contact. Liquid water is boiled off and steam enters the bottom of a tank containing the plants from which the essential oil needs to be extracted, these plants forming a porous medium of given compaction. The vapour can be simply saturated, or generated in an independent circuit allowing for the production of superheated steam, which is more complex but can increase the extraction speed and reduce the hydrolysis problem.

In both cases, the temperature increase of the plants and the presence of water allow the oils diffusing towards the surface of the plants and evaporating to be carried away by the vapour flow rate [5]. Because this extraction technique has the widest applications while being the simplest to implement, this work focusses on the **steam distillation process using saturated water vapour**. This technique suits most of the plants of which the oils are secreted by cells situated in the leaves (inside the tissue or at the surface).

1.3.2 Parts of an Extractor using Steam Distillation

A classical extractor for essential oils using steam distillation, whose global configuration is shown on figure 1.2, comprises two main parts: the extraction system, composed of a plants tank, a condensing unit and a separator, and the steam generation system. These elements are described below, with the associated design constraints:

- **Extraction system**

Plants tank Containing the plants, its shape is generally cylindrical, as the best compromise between the ease of handling, charging, emptying and cleaning it on the one hand, and the required uniform distribution of steam across the plants bed cross-section. Nevertheless, a distributor such as a fine grid must be placed at the bottom of the plants bed to help homogenising the steam flow across the cross-section.
The bottom and top of the tank are pierced in order to respectively allow for the entrance of steam and the evacuation of the vapour. Apart from those two openings, the whole system must be perfectly watertight. The exit nozzle at the top of the tank must be short in height and insulated to avoid any back-flow due to condensation.
The thermal insulation of the tank walls and cover is generally necessary to restrain the fraction of the vapour flow rate condensing in the tank. A too important condensation involves an increase of steam consumption, an increase of the extraction duration and even a decrease of the efficiency[4]. Nevertheless, a certain level of wetting is necessary to allow for the diffusion of the essential oil from its secreting cells towards the plants surface.

Condensing unit It is generally constituted of a long conductive pipe bended in a spiral or zigzag form, processing the vapour flow exiting the tank. The pipe is immersed in a (usually) circulating cooling fluid (generally water). The forced convection operated by the flow of cold water allows to efficiently condensate and cool down the substrate, which exits the condensing unit under the form of a two-phase liquid.

Separator In most cases, the density of the compounds of the essential oil is lower than the density of water. The separator, located at the exit of the condensing unit, is thus generally conceived on the basis of this property. Thanks to a syphon system, the water phase can be evacuated throughout the bottom of the separator and collected in an other container, while the essential oil accumulates in the separator.

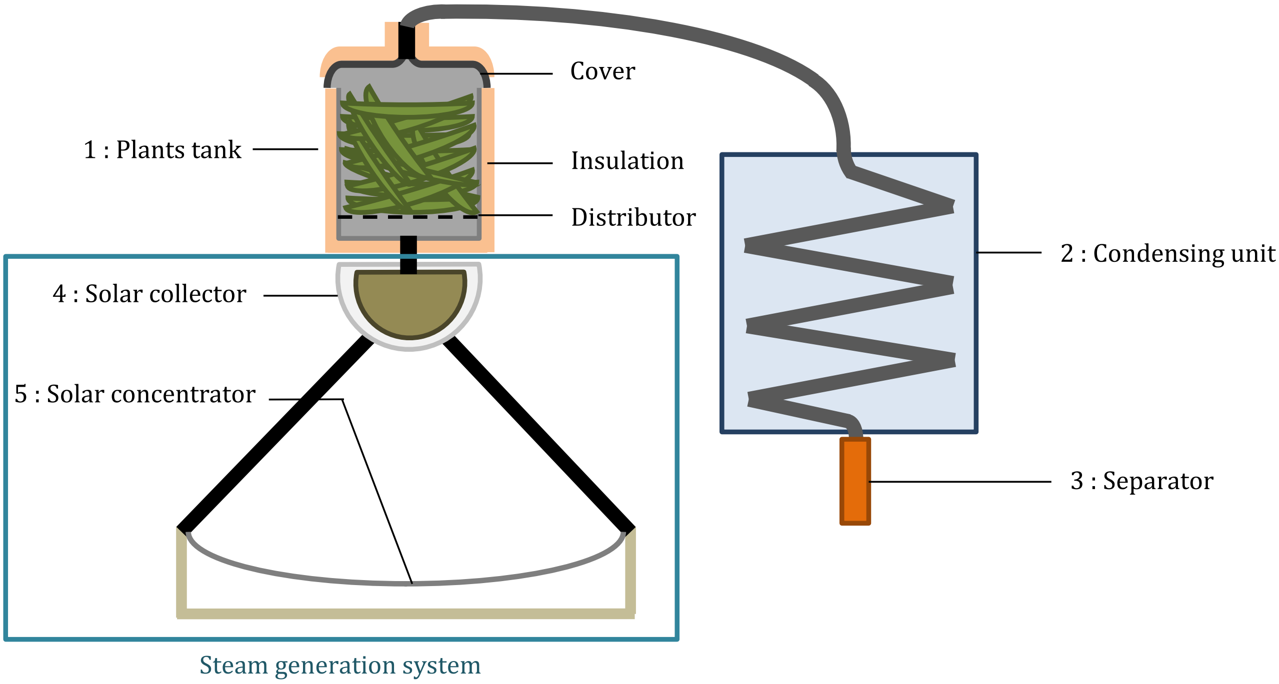

Figure 1.2: Global configuration of a steam distillation extraction unit

[4]The efficiency of an extraction of essential oil is defined in literature as the ratio of the quantity of collected oils (in mL) by the mass of plants (fresh or dry, depending on the author) put in the tank. [6]

- **Steam generation system** Saturated steam is generated by heating and boiling off water placed in a container below the tank. Any heating source would work, but one of the purposes of this work is to exploit the availability of solar energy in Burkina Faso, in a sustainable development perspective. Therefore, a solar concentrator can be used to reflect the solar radiation towards the water container, playing the role of a solar collector.

1.3.3 Causes of Variation of Oils Composition, Extraction Efficiency and Duration

Finally, for a same aromatic species under the process of steam distillation extraction, the composition of the extracted oils, the extraction efficiency and the extraction duration are three characteristics representative of the success of a given extraction. Numerous factors influence them:

Picking and pre-processing of the plants Several pre-processing steps have to be applied to the plants before starting extracting the oils from them. When considering the wide case of leaves, the following have shown to have an influence: growing place, picking time (period of the year and moment of the day), physiological state of the leaves (age and flowering state), hydration level, drying duration and conditions [6], [19].

Chopping degree of the leaves and bed homogeneity Chopping the leaves allows increasing the exchange surface and admitting a shorter extraction duration and a better efficiency. However, the chopping process can induce the thermal degradation of some components of the oils and losses by volatilisation. Also, the bed granulometry cannot be too fine nor inhomogeneous to avoid the occurrence of preferential paths in the plants bed that would reduce the homogeneity of the steam distribution [5], [6].

Superficial speed of steam through the plants bed Previous studies conducted in laboratory [6] state that the optimal superficial speed of steam is comprised between two boundaries. The lower boundary corresponds to the superficial speed under which steam cannot impregnate the plants bed in an homogeneous way, for a given type of plants bed. The upper boundary is such that the ratio between waste water and collected oils at the exit of the condensing unit is too high and leads to the dissolution of certain oils compounds in the waste water, this corresponding to a modification of the oils composition and a decrease of the extraction efficiency [23].

Materials and design characteristics of the extractor It is important that the materials of the extractor do not contaminate the extracted oils, as this directly influences their composition and quality. The oils compounds are organic, with various chemical functions depending on the plant type. The interactions and compatibility of this type of compounds with the possible materials of the extractor must therefore be verified. Also, as mentioned in the previous subsection, design parameters such as the tank shape or the type and configuration of the tank insulation are important.

These last two points are particularly important in the framework of this thesis.

Chapter 2

Objectives

The global objective of this work is to contribute to the inter-university cooperation between the Université libre de Bruxelles to the Université de Ouagadougou, focussing on the extraction process of essential oils using steam distillation and solar energy. This global objective involves three specific objectives described here below.

Objective 1: Selection of construction materials for all parts of the extraction unit There are several constraints determining the materials selection of an extraction unit for essential oils using steam distillation and solar energy. First, they must be adapted to the dimensions and environment of the unit. For example, glass is ideal for an indoor extraction unit of small size, but is not suited for an outdoor unit of large dimensions. Second, they must be durable, i.e. the unit cannot undergo wear under normal use, neither by its environment nor by the products that it contains and processes. Third, they may not in any way contaminate the products of the distillation. This is indeed the main requirement for the production of essential oils (as stated in section 1.2). Finally, they must be available on the site of construction, preferably at a competitive price (the cost limitation is of course a major point).

Objective 2: Sizing of the extraction unit A rational sizing of all parts of the extraction unit allows optimising the extraction efficiency and reduce the extraction duration. Indeed, it was mentioned in subsection 1.3.3 that the superficial speed of steam through the plants bed must be comprised between two known boundaries. Therefore, a model of the heat transfers occurring in each part of the extraction unit is established.

Objective 3: Construction of the extraction unit in Ouagadougou This objective relies on the results of objectives 1 and 2. It first involves the elaboration of a construction strategy with Adama Ouedraogo, in charge of the Atelier Central de Maintenance (ACM, central maintenance workshop) of the Université de Ouagadougou. Then, the ordering of the raw materials locally and the construction of the extraction unit in collaboration with the staff of the ACM.

Objectives 1 and 2 constitute a preliminary study of the extraction unit, which is presented in chapter 3. The realisation of objective 3 is presented in chapter 4.

Chapter 3

Preliminary Study of the Extractor

3.1 Materials Selection

3.1.1 Objectives

In the framework of inter-university cooperation between the Université libre de Bruxelles (ULB) and the Université the Ouagadougou, an extraction unit was built in 2009 by a team of ULB Master students. However, the oils produced upon studies about characterisation of the extraction process of *Eucalyptus Camaldulensis* oils [6], [32], showed a poor quality, as indicated by the dark brown colour instead of light yellow of the oils. This means that the composition of the oils was altered, possibly through interactions with the extractor materials.

The following table compiles the list of materials used for each subsystem upon the construction and improvements of the existing extraction unit at the Université de Ouagadougou. For some of the subsystems, the material type is assessed from its visual properties, and most of the time the alloy or exact composition is unknown. The data are recent (state of the unit at the moment of the author's stay in Ouagadougou, March 2013).

	Subsystem	**Material**
1	Plants tank	aluminium - alloy or purity unknown
2	Insulation	glass wool
3	Water container	low carbon steel
4	Condensing pipes	stainless steel
	Connectors	copper or galvanised steel
5	Condensing tank	low carbon steel
6	Seals	red cardboard (?)

There are several possible causes that could explain the abnormal colour:

- Presence of dissolved Iron ions (Fe^{3+}) in the oils. Indeed, these ions give a red colouration to aqueous solutions. They could originate from the dissolution of rust forming in the galvanised steel connectors, possibly weathered at the time of the extractions through an extended contact with water. Also, one of the galvanised steel connectors was submitted to welding to ensure that the connection is watertight, which most certainly damaged the protective zinc layer and brought welding metal (probably steel). This connector is however situated below the plants tank, and the iron ions are probably too heavy to be carried away by steam against gravity.

- Interaction between the oils and the seals, giving their reddish colour (see figure 3.1) to the oils.

Figure 3.1: Reddish colour of the old gaskets

Moreover, the presence of a metallic deposit in the extraction products was observed during previous studies [32]. It was identified as originating from interactions between the essential oil and the copper parts (condensing pipes and connectors) of the extraction unit, as the same deposit was observable on the copper elements after each extraction (see figure 3.2). At the beginning of the studies of 2012, the condensing pipes were entirely replaced by stainless steel, this improvement allowing to suppress the main source of copper deposit in the extraction products. Although some copper connectors remained, the metallic deposit was not mentioned any longer [6].

(a) Deposit on altered connector (b) Deposit in extraction products

Figure 3.2: Metallic deposit originating from interactions between essential oil and copper

The main objective of the materials selection is thus to provide a list of materials for all parts of the extraction unit, that are compatible, amongst other process constraints, with the compounds of essential oils, in order to allow for a **cleaner production of oils**

3.1.2 Methodology

The methodology adopted to determine the materials of all parts of the extraction unit is the following:

The extraction unit is divided into subsystems. To each subsystem are associated its function and the characteristics of the environment it is interacting with (temperature, pressure, substance, phase, etc.). From there, a list of requirements and constraints regarding the thermal, mechanical, corrosion and durability properties of the material is established, finally allowing the determination of the criteria for the materials selection, which is performed using the Cambridge Engineering Selector (CES) Edupack, constituting a vast database for materials and their various properties (thermal, mechanical, durability, etc.). The critical review of the results allows rejecting the bad candidates and, at the end, a list of possible materials choices is recommended.

3.1.2.1 Definition of the Subsystems

As far as the materials selection is concerned, the extraction unit can be divided into six distinct subsystems:

1. **Plants tank** containing the plants raw material.
2. **Insulation** placed around the plants tank to limit heat losses and steam condensation across the plants bed.
3. **Water container** part of the steam generation system, containing boiling water.
4. **Condensing pipes and connectors** conveying the extraction products or steam between or through the different parts of the extraction unit.
5. **Condensing tank** containing cooling fluid for the condensation of the extraction products.
6. **Seals** insuring the tightness of the connections between removable parts.

3.1.3 Selection

3.1.3.1 Global Criteria

Global (to be considered for all parts of the system) criteria are priorly defined :

Price is always crucial in a value engineering perspective. It is even more in the framework of a development cooperation project. Indeed, a low cost oriented design enables an easier production of the device afterwards, allowing wider use.

Density For large components of the extraction unit, the minimisation of the materials density eases the handling and maintenance of the device during its whole life .

Fracture toughness A maximisation of the fracture toughness allows increasing the device lifetime. Indeed, the outdoor environment and the relatively large dimensions of the extraction unit prohibits the use of too fragile materials.

Availability It is expected that very specific materials, requiring for example particular manufacturing techniques, will not be available in Burkina Faso. However, the materials selection considers all possibilities, considering that the materials availability is going to be assessed on site.

These criteria are not repeated in the following sections, as it is implied that they apply.

3.1.3.2 Plants Tank

1. **Function**: container for the plants bed. Secondary: limits vapour condensation[1].

2. **Environment**: plant raw material, water (vapour and liquid), essential oil (vapour and liquid). Its inner walls temperature (the hottest) can reach 100°C (boiling water temperature). Since saturated vapour is generated, the pressure is ambient (around 1 atm). Therefore, pressure is not a constraint. The plants tank is surrounded by a layer of insulation material, constituting a protection against the outside environment.

3. **Requirements and constraints**: resistance of the material to the temperature conditions imposed by its environment, no chemical interactions between the material of the plants tank and its environment (durability of the material and no contamination of the oils extracted). Optional: insulating material.

4. **Criteria**:

   - Maximum service temperature above 120°C. A margin is taken with respect to the boiling temperature of water.
   - Excellent durability with respect to fresh water[2].
   - Excellent durability with respect to essential oils. This specific durability property is not provided by the CES software. However, the durability properties with respect to numerous solvents and oils are provided, and this gives a first idea of whether to reject a material a priori. However, further investigations are needed for all the good candidates of the selection.
   - Minimisation of the thermal conductivity (optional).

The application of all limiting criteria eliminates an important part of the materials, and finally allows investigating the following candidates (see figure 3.3 of the remaining candidates, plotted on a graph of thermal conductivity as a function of price):

Non-technical ceramics such as brick: despite their exceptional durability and their cheap price, the principal reason for rejecting this category of materials is their bad processability. Indeed, as said in section 1.3, the plants tank shape should be cylindrical to allow steam homogenisation across the bed. Moreover, some of those materials are porous.

Phenolics this category of materials is one of the only polymers groups outlasting the thermal constraint. An investigation of its industrial applications shows that it is often used for the storage of corrosive and organic substances, which allows thinking a priori that it would not interact with the essential oils. Indeed, this is confirmed by the compatibility table provided in the Valspar catalog, which reviews numerous organic compounds including essential oils [27]. Moreover, its insulating properties are interesting in the purpose of limiting the condensation in the plants tank and removing the need for an additional insulation layer. Finally, it presents good moldability properties, low density and relatively cheap price. However, the availability of this type of materials seems to be the principal concern. It is possible to find manufacturers of phenolics in Europe, but they mostly produce it under the form of coatings for industrial purposes [27]. Even if some

[1] It is worth noting that two strategies can be adopted with regard to the limitation of condensing phenomena of vapour inside the bed: build the plants tank using an insulating material or add an insulating layer around the plants tank.

[2] The CES Edupack software allows distinguishing fresh from salt water, with regard to the materials durability properties

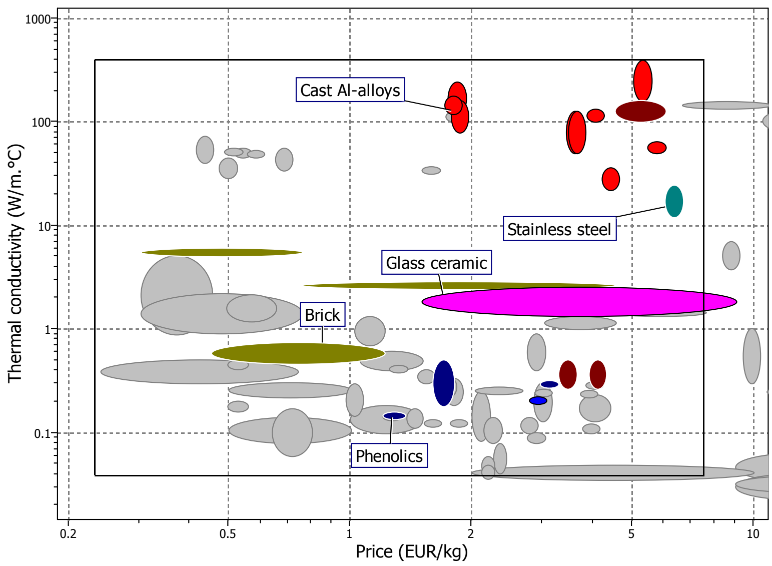

Figure 3.3: Last step of the material selection for the plants tank

steel tanks coated with phenolics were found online, the choice in dimensions remained narrow. Therefore it is expected that phenolics will not be available in Burkina Faso.

Glass ceramics its excellent durability properties are attractive. Besides, glass (more precisely borosilicate glass, having the same durability properties as glass ceramics) is usually used for the small extraction units mounted in laboratory. However, the still high brittleness of glass ceramics (even if it is lower than the brittleness of common borosilicate glass) constitutes a risk, accentuated by the fact that the plants tank would have to be manufactured in one piece to ensure that the system is watertight. Nevertheless, the processability of glass ceramics is limited.

Aluminium alloys it is the cheapest alternative within the metals family. Like other metals, it benefits from good mechanical properties, having high fracture toughness, high yield strength and being ductile. Moreover, aluminium is known for its good water durability. However, its durability with respect to essential oils is unknown.

Stainless steel very expensive, but it is a reliable (probably the best) choice with respect to material durability and non-contamination of the products.

3.1.3.3 Insulation

1. **Function**: insulating the plants tank walls, the plants tank cover and the necessary connections.

2. **Environment**: possible contacts with water while handling the extraction unit. As the insulation layer is in contact with the plants tank, its inner surface could reach temperatures approaching 100°C. The outside environment involves an important solar exposure.

3. **Requirements and constraints**: insulating material, no thermal degradation of the insulating properties within the range imposed by its environment, no degradation of the insulating properties by water, flexible as the insulating layer is meant to be wrapped around the cylindrical tank and other connectors of small diameters, resistant to sunlight exposure as this layer is external.

4. **Criteria**:

    - Minimisation of the thermal conductivity.
    - Maximum service temperature above 110°C. A margin is taken with respect to the boiling temperature of water.
    - Excellent durability with respect to fresh water.
    - Flexural modulus inferior to 1 GPa[3].
    - Good or excellent resistance to sunlight exposure (UV radiations).

The application of all limiting criteria eliminates an important part of the materials, and finally allows examining the following candidates:

Glass foam this is a common insulating material for walls, pipework, tanks [12].

Phenolic foam another material widely used for thermal insulation applications.

Vermiculite its primary application is in sound insulation.

3.1.3.4 Water Container

1. **Function**: containing the water to be boiled off.

2. **Environment**: fresh water (liquid and vapour). Residues of organic substances through a flow-back coming from the bottom of the plants tank. Its walls could reach very high temperatures, as they absorb concentrated solar radiation directed towards the water container by the solar concentrator.

3. **Requirements and constraints**: conductive material to provide as much heat as possible to the heated fluid, durable with respect to fresh water and organic components (NB: here, the concern is mostly to preserve the container from wear and degradation. Indeed, even if metallic ions were dissolved in water, they would be too heavy to be carried away with steam[4] towards the plants bed. There is thus no risk of contamination.), high thermal resistance.

4. **Criteria**:

    - Maximisation of the thermal conductivity.
    - Maximum service temperature above 150°C. It is indeed expected that the water container will reach very high temperatures, as it receives the concentrated solar radiations reflected by the parabola.
    - Excellent durability with respect to fresh water.
    - Good or excellent resistance to sunlight exposure (UV radiations).

The best candidates passing all stages of the materials selection are the set of **Aluminium alloys** (see figure 3.4 of thermal conductivity as a function of price). Indeed, they are the lightest while being highly conductive and affordable. Their good properties with respect to

[3] The flexural modulus corresponds to the stiffness in bending of a material. The CES design note for flexural modulus gives flexural modulus classes by increasing values, with the corresponding materials properties; a flexural modulus inferior to 1 GPa corresponds to «Flexible plastics and elastomers» [12].

[4] The carryover of metallic solutes in steam occurs at high pressures (above 16 bars) only, for which the steam volatility of diverse compounds increases significantly [15].

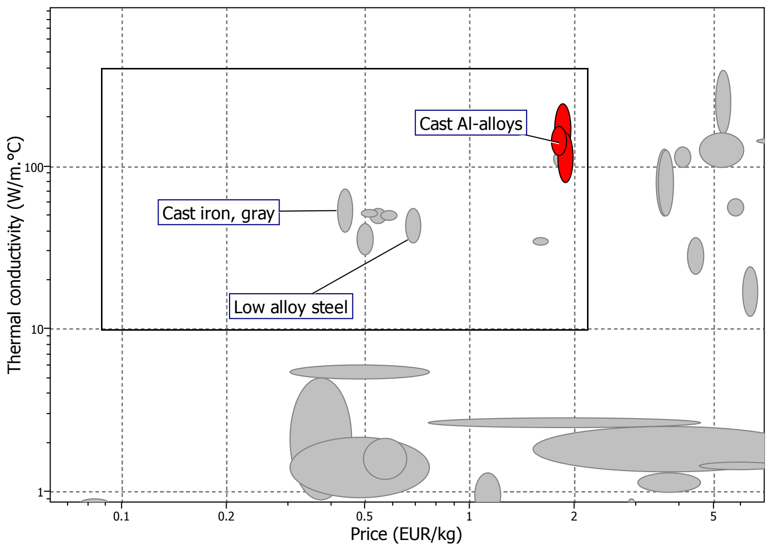

Figure 3.4: Last step of the material selection for the water container

water are ensured by the formation of a protective layer of aluminium oxide at the surface of a given sample. This layer forms at the contact with air and is insoluble in water, preventing thus the propagation of corrosion deeper inside the sample [29]. A further investigation of the different alloys of aluminium allows retaining the family 5052 as an interesting candidate. Indeed, this class of aluminium alloys is recommended for sheet metal work applications, where «good workability, very good resistance to corrosion, weldability and moderate static strength are desired» [12].
It is worth noting that low alloy steels, low, medium or high carbon steels and irons are eliminated because of their bad durability properties with respect to water (tendency to rusting). However, they are cheap and conductive, and most of all very common and therefore probably available on site.

3.1.3.5 Condensing Pipes and Connectors

The following analysis (function, environment, requirements and constraints and criteria) is conducted for the condensing pipes, but the selection results can be extended to all connectors of the extraction unit. Indeed, connectors are small pipework pieces in contact with globally the same substances as the condensing pipes.

1. **Function**: process the distillation products towards the exit of the condensing unit while favouring the heat exchanges between the distillation products and the water contained in the condensing tank.

2. **Environment**: essential oils and water (vapour and liquid) inside and liquid water outside. The maximum temperature of the pipes walls is around 100°C.

3. **Requirements and constraints**: conductive material in order to facilitate the heat exchanges through the pipes walls, durable with respect to water and essential oils.

4. **Criteria**:

   - Maximisation of the thermal conductivity.
   - Maximum service temperature above 110°C.
   - Excellent durability with respect to fresh water.

- Excellent durability with respect to essential oils.

The materials selection leads to the following short list, to be further considered as materials for the condensing pipes:

Aluminium alloys Good conductivity properties, light, cheap, resistant to water. However, as already mentioned, their durability properties with respect to essential oils are unknown.

Chromium-steel alloys Apparently available on site and relatively cheap [6]. However, the durability properties are unknown, mostly because the exact composition of the alloy is unknown.

Stainless steel Safe choice with respect to the durability concerns, but expensive.

3.1.3.6 Condensing Tank

1. **Function**: contain the water that plays the role of the cooling fluid of the condensing unit. Therefore, the condensing tank material must ease the evacuation of the condensing heat towards the outside environment.

2. **Environment**: liquid water. As a first estimation, the tank walls would reach temperatures of maximum 60°C.

3. **Requirements and constraints**: conductive material to facilitate the heat exchanges towards the outside environment, durable with respect to water (NB: as the condensing tank does not interact with the distillation products, there is no contamination concern. Moreover, the tank is very accessible and of simple geometry, which makes its maintenance very easy if necessary (renewing of the painting or a coating for example.)).

4. **Criteria**:

    - Maximisation of the thermal conductivity.
    - Maximum service temperature above 60°C.
    - Acceptable or excellent durability with respect to fresh water.
    - Good or excellent resistance to sunlight exposure (UV radiations).

The best alternative is again the set of **Aluminium alloys**. Their good durability properties with respect to water eliminates the need for any coating or painting and therefore any maintenance during the extraction unit lifetime. However, it is still possible to use a tank made out of **Iron** or **Steel** and treat it regularly with anti-rust coatings.

3.1.3.7 Seals

Flat gaskets are needed to ensure the tightness of the whole extraction unit, especially at the connections between piping elements, that need to be assembled and disassembled regularly for cleaning and storage of the unit. A large size seal is also needed to ensure the tightness between the plants tank and its cover, which is also often opened and closed to allow for the plants filling.

1. **Function**: ensure that the piping connections are watertight.

2. **Environment**: water and essential oils (liquid and vapour). Some of the seals can reach temperatures up to around 100°C.

3. **Requirements and constraints**: resistance of the material to the temperature conditions imposed by its environment, no chemical interactions between the material of the plants tank and its environment (durability of the material and no contamination of the oils extracted), maximum conformability (i.e. maximisation of the contact surface between gasket and mating surfaces), limit on contact pressure [2].

4. **Criteria**:

   - Maximum service temperature above 110°C.
   - Excellent durability with respect to fresh water.
   - Excellent durability with respect to essential oils.
   - Maximisation of the index ${\sigma_f}^{1.5}/E$ to allow for maximum conformability [2], with σ_f the failure strength, corresponding here to the yield strength as the gasket must remain elastic to fulfil its role properly, and E the Young's modulus. The maximisation of the index is performed by drawing a line of slope 2/3 on the bi-logarithmic graph of σ_f versus E and selecting the materials above the line (see figure 3.5).
   - Maximisation of the index $1/E$ to limit the contact pressure, i.e. to ensure that the gasket is more malleable than the mating surfaces [2].

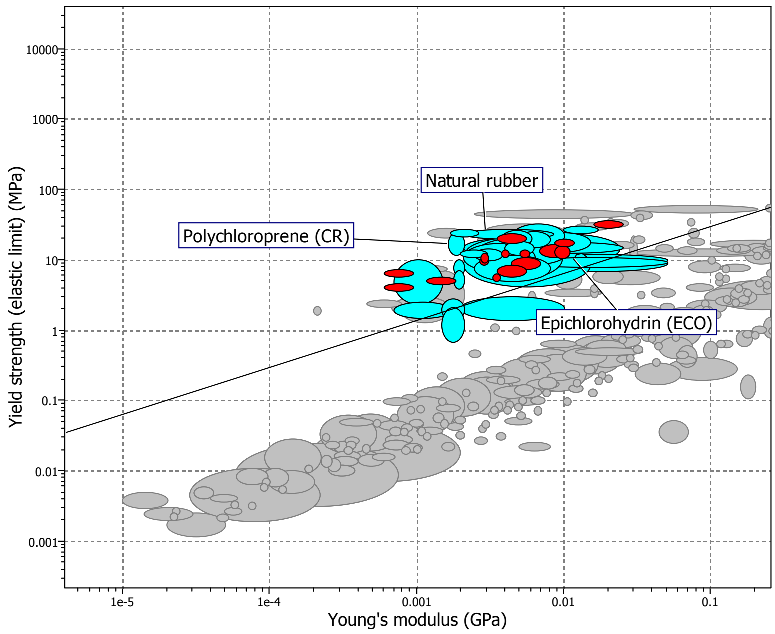

Figure 3.5: Material selection for seals - the blue sets are thermoset elastomers and the red sets are thermoplastic elastomers

As shown on figure 3.5, numerous elastomers fulfil the selection criteria. However, the compatibility of each of them with respect to essential oils still needs to be verified. Here below, three examples of candidates are analysed:

Natural rubber (NB) excellent mechanical properties and high fatigue resistance, while being cheap. However, natural rubber presents very bad durability properties with respect to oils and hydrocarbon fluids [12]. Benjilali confirms that natural rubber is partially soluble in essential oils and therefore should be avoided [5].

Polychloroprene (CR) very good mechanical properties and fatigue resistance, while being cheap. Its durability properties with respect to oils are better than those of natural rubber. However, Marston rates CR as «3 - poor: performance depends on required life and level of chemical» with respect to aromatic hydrocarbons in its chemical resistance table [22].

Epichlorohydrin (ECO) a noted alternative to natural rubber in case resistance to solvent is required. This is confirmed by Marston, rating ECO as «1 - good: satisfactory performance in relatively high level of chemical» with respect to aromatic hydrocarbons in its chemical resistance table, which corresponds to the highest rating available for the series of rated elastomers [22].

Besides flat seals, a material is needed to cover the thread of the connectors and ensure the adherence of the two threaded parts. For this purpose, Polytetrafluoroethylene (PTFE), commonly known as Teflon, presents an excellent resistance against corrosion and is cheap. Its compatibility with respect to essential oils is confirmed by its rating with respect to aromatic hydrocarbons given by Marston: 1 (the best rating) [22].

3.1.4 Corrosion Properties of Metals

Metallic candidates are numerous, for almost every subsystems of the extraction unit. It is interesting to investigate further their corrosion properties before making a final recommendation about the materials.

Cast iron and Carbon steel (variable carbon composition) : in contact with air and water, formation of a layer of iron (Fe^{3+}) oxide (rusting). This layer is not protective, i.e. the rusting phenomenon continues propagating until the whole part is oxidised. Moreover, iron oxide layers are brittle, which accelerate the deterioration.

Stainless steel (Carbon steel + minimum 10.5% chromium (Cr) [12]) : in contact with air, auto-generation of a passive protective layer of chromium. If this layer is not damaged, it indefinitely protects the material against corrosion. However, if the medium in contact with the material is respectively acidic or highly concentrated in chloride, corrosion can be instigated, leading to generalised or localised (e.g. pitting) deterioration of the material [13].

Chromium steel (Carbon steel + less than 5% chromium [12]) : the content in chromium being lower, it is expected that the general corrosion properties of chromium steel will be inferior to those of stainless steel. However, they are superior to those of carbon steel.

Aluminium and derived alloys : when first in contact with air, a layer of water insoluble aluminium oxides forms at the surface of a given sample. The protective layer is self-renewing. If the layer, stable for neutral pH, is not damaged, it indefinitely protects the material against corrosion. However, if the medium in contact with the sample contains heavy metals or high chloride concentrations, the sample undergoes pitting. If it is acidic (pH below 4.5), the layer of aluminium oxides becomes unstable, leading to generalised corrosion [20], [29]. It is worth noting that Benjilali indeed recommends the use of aluminium for the condensing pipes of extracting units for essential oils, except if the products contain phenols, that are midly acidic organic compounds [5].

Copper : at the contact with clean atmosphere, copper develops a green adherent oxide layer at its surface. The latter allows copper to have good corrosion properties in atmospheric conditions [12]. However, copper is known to alter the colour of essential oils [5], probably because of interactions between copper oxides and some compounds of the oils.

Zinc Pure zinc is widely used as protective coatings for steel in numerous applications, particularly outdoor to prevent the natural degradation of steel. This is the purpose of galvanisation: the zinc layer of galvanised samples acts as a sacrificial coating, corroding instead of steel in the presence of water [12]. Moreover, zinc resists well mildly acidic media. Besides, Benjilali recommends the use of galvanised steel for the plants tanks of units extracting oils containing acidic compounds [5].

3.1.5 Conclusion

The following table presents for each subsystem a final recommendation regarding the materials. There is always a compromise to be made between quality, durability and costs reduction. The selection of optimal materials wishes to give priority to quality and durability. However, the compatibility between essential oils and the diverse materials is difficult to assess, it is not widely approached in literature and it depends on the composition of the oils. Therefore, it is worth keeping some of the cheaper and more risky alternatives in mind, and make the final choice on site, in view of the availability and possible alternatives.

	Subsystem	**First choice**	**Alternative**
1	Plants tank	Steal coated with phenolics or Stainless steel	Aluminium
2	Insulation	Glass foam	any available
3	Water container	Aluminium 5052	Carbon steel
4	Condensing pipes and connectors	Stainless steel	Chromium steel
5	Condensing tank	Aluminium 5052	Carbon steel
6	Seals	Epichlorohydrin and Polytetrafluoroethylene	any available and fulfilling the criteria

3.2 Sizing

3.2.1 Notations

The notations used in the following subsections are presented in table 3.1, with the corresponding units, significations and often reoccurring indices.

Symbol	Unit	Signification	Often reoccurring indices
g	m/s^2	gravity constant	
σ	W.(m.K^2)$^{-2}$	Stefan-Boltzmann constant	
M	kg	mass	p: plants; w: water
ρ	kg.m^{-3}	density	w: water; vap: vapour; liq: liquid
t_{ext}	s	extraction time	
D	kg/s	mass flow rate	vap: vapour
V	m/s	superficial speed	vap: vapour
d	m	diameter	
r	m	radius	
L	m	length	p: parabola
e	m	thickness	
H	m	height	
S	m^2	surface	p: parabola
T	K	temperature	atm: atmospheric
p	atm	pressure	atm: atmospheric
h	W.(m^2.K)$^{-1}$	heat transfer coefficient	r: radiation; conv: natural or free convection; fconv: forced convection; mconv: mixed convection;cond: conduction
k	W.(m.K)$^{-1}$	thermal conductivity	f: fluid; s: solid;
R	K/W	thermal resistance	
Q	W	heat flux	
q	W.m^{-2}	heat flux density	cf. h
F	W.m^{-2}	flux density	none: solar; p: reflected by parabola
a	-	absorptivity	specific to each material
ε	-	emissivity	specific to each material
η	-	overall efficiency	
Pr	-	Prandtl number	
Bi	-	Biot number	x: characteristic dimension
Gr	-	Grashof number	x: characteristic dimension
Ra	-	Raleigh number	x: characteristic dimension
Nu	-	Nusselt number	x: characteristic dimension
C_{p}	W.(kg.K)$^{-1}$	specific heat capacity	
L_{vap}	W/kg	latent heat of vaporisation	
ν	m^2/s	kinematic viscosity	
μ	P.s	dynamic viscosity	
β	K^{-1}	volumetric expansion coefficient	

Table 3.1: Notations

3.2.2 The Heat Transfer Theory

A temperature difference between two given media put in contact causes several heat transfer mechanisms to take place, tending towards an equilibrium. In this section, the different heat transfer modes are briefly reviewed, with the corresponding non-dimensional numbers.
There are three main heat transfer modes:

Radiation Radiation is a transfer of energy that occurs between distant bodies (solid, liquid or gas), through electromagnetic waves [8].

Conduction Conduction occurs in solids or stationary fluids, by the microscopic movements of the medium molecules or atoms. The conduction heat flux density is proportional to the temperature gradient within the medium, through a conductivity coefficient characteristic of each material/fluid [8].

Convection Convection occurs in fluids in contact with a solid wall, through the combination of conduction and advection (macroscopic movements of fluid molecules). In the case of natural convection, these movements are caused by the temperature difference between fluid and solid, and the resulting differences in fluid density between the warmer and colder regions. On the other hand, forced convection is instigated by fluid movements that are independent on the temperature difference and result from an outside action [8].

The last two heat transfer modes are associated to several non-dimensional numbers, defined bellow with the corresponding formula, that will be used in the following sections:

- **Prandtl number (Pr)** (conduction in fluids) It compares the diffusive mechanisms of momentum and heat, and assesses the distortion existing between the two phenomenons. It is given by the ratio $\frac{\nu}{\alpha}$, with ν the fluid kinematic viscosity. The thermal diffusivity is expressed as $\alpha = \frac{k}{\rho C_{\mathrm{p}}}$ and compares the capacity to transfer heat by conduction with the capacity to store it [8].

- **Biot number (Bi)** (conduction-convection) It gives the ratio between thermal resistances inside and at the surface of a body (index s): $\mathrm{Bi}_{x_s} = \frac{hx_{\mathrm{s}}}{k_{\mathrm{s}}}$. If $\mathrm{Bi} \leq 1$, a block behaviour can be associated to the body with regard to its temperature, i.e. its temperature is considered uniform across its characteristic dimension [8].

- **Nusselt number (Nu)** (convection) It gives the ratio of convective to conductive heat transfer at the boundary of a solid with a fluid, the conductive heat transfer being computed under the same conditions but considering a stationary fluid (index l): $\mathrm{Nu}_{x_{\mathrm{l}}} = \frac{hx_{\mathrm{l}}}{k_{\mathrm{l}}}$ [8].

- **Grasshof number (Gr)** (natural convection) It compares the floating effect induced by the Archimed force with the resistive effect caused by viscous shear. In the case of an isothermal wall of temperature T_w put in a fluid of temperature T_f, it is given by $\mathrm{Gr}_x = g\beta x^3 \frac{T_{\mathrm{w}} - T_{\mathrm{f}}}{\nu^2}$, with β, ν characteristic of the surrounding fluid. On the other hand, if the heat flux through the wall of thermal conductivity k_w is constant and equal to q_{w}, then $\mathrm{Gr}_{\mathrm{x}} = \frac{g\beta x^3}{\nu^2} \frac{q_{\mathrm{w}}}{k_{\mathrm{w}}}$ [8].

- **Raleigh number (Ra)** (natural convection) It is given by $\mathrm{Ra}_x = \mathrm{Pr}\mathrm{Gr}_x$ [8].

- **Richardson number (Ri)** (natural-forced convection) It compares the relative importance of free and forced convection. It is given by $\frac{\mathrm{Gr}}{\mathrm{Re}^2}$. If it is $\simeq 1$, the convection is mixed, if it is $\ll 1$, the convection is mostly forced, and if it is $\gg 1$, the convection is mostly natural [8].

Finally, the computation of the radiative heat transfers between a body and the atmosphere requires the assessment of the **sky temperature**, the sky being considered as a black radiator[5]. The sky temperature $T_{\text{sky}}[K]$, always between 5 and 30 K below the ambient temperature, depends on the dew point temperature $T_{\text{dp}}[°C]$ of air and the ground air temperature $T_{\text{atm}}[K]$ in the following way, with t the hour after midnight [21]:

$$T_{\text{sky}} = T_{\text{atm}}\Big[0.711 + 0.0056T_{\text{dp}} + 7.3 \times 10^{-5}{T_{\text{dp}}}^2 + 0.013\cos\left(2\pi t/24\right)\Big]^{1/4} \tag{3.1}$$

The dew point temperature depends on the relative humidity of air RH (non-dimensional), and is given by the following correlation [31]:

$$T_{\text{dp}}[°C] = \frac{b\gamma}{a-\gamma} \tag{3.2}$$

with $a = 17.27$, $b = 237.3$ and $\gamma = \frac{aT_{\text{atm}}[°C]}{b+T_{\text{atm}}[°C]} + \ln(RH)$

3.2.3 Sizing Objectives and Methodology

As seen in section 1.3.3, a crucial parameter of the extraction process acting on its efficiency, its duration and the quality of the oil extracted is the superficial speed of steam through the plants bed. The goal of this section is to elaborate a model of the extraction unit allowing to size it properly on the basis of imposed or required data, such as the superficial speed of steam, the extraction duration and the mass of plants to be processed. At the end of the sizing, two main parameters need to be determined:

1. the area of solar reflecting surface required such that it allows for the generation of the required superficial speed of steam, for a given plants tank diameter,
2. the area of condensing pipes allowing for the condensation and cooling of the vapour flow rate entering the condensing unit.

The determination of these two main parameters requires the determination of several intermediate parameters.

The methodology adopted for the sizing of the extractor is the following:

First, several subsystems are defined in relation to the heat exchanges. Then, the heat exchanges occurring in each subsystem are modelled using different balances, such that the number of unknowns corresponds to the number of equations to solve. For this purpose, a number of assumptions need to be made through the whole process, regarding e.g. coefficient values, heat exchanges modes and negligible phenomena. The output variables of a subsystem are the input variables of the next. Each subsystem is solved thanks to the implementation of Matlab codes based on the balances and assumptions.

3.2.3.1 Definition of the Subsystems

The extraction unit can be divided into four distinct subsystems with regard to the sizing:

1. **Solar concentrator** - also called **parabola** in the following sections
2. **Solar collector** - composed of the water container surrounded by a greenhouse

[5]The intensity and specific spectrum of radiation emitted by a black radiator only depends on its temperature, and not of its shape or composition.

3. **Plants tank**

4. **Condensing unit**

3.2.4 Modelling the Heat Exchanges

3.2.4.1 Predeterminations

As stated in section 1.3.3, studies conducted in laboratory allowed determining the range of heating powers (which are directly related to the superficial speed of steam across the plants bed) such that the extraction is well performed, for the dimensions and design of the extraction unit available at the TIPs laboratory of the ULB[6] [6]. Beyond the two boundaries, problems of efficiency, extraction duration and oils quality arise. The lower boundary corresponds to the superficial speed under which steam cannot impregnate the plants bed in an homogeneous way. In other words, steam takes preferential paths to cross the bed, and entire regions of the plants bed are not reached by water, causing the corresponding essential oil content to stay unextracted. It is thus particularly important to always stay above this lower boundary. On the other hand, the upper boundary is such that the ratio between waste water and collected oil at the exit of the condensing unit is too high and leads to the dissolution of certain oil compounds in the waste water, this corresponding to a modification of the oils composition and a decrease of the extraction efficiency [23]. Moreover, staying below the upper boundary allows limiting water consumption, which is not negligible in countries with dry climatic conditions like Burkina Faso.
On the basis of these results, a value of the heating power P_{m} is chosen in the middle of the interval determined in laboratory, to ensure being as far from the boundaries as possible. This value allows computing the required steam superficial speed that should be available across the plants bed, which is the same in the lab and on site.

First, if the assumption is made that all the heating power provided to the laboratory water container is used to evaporate water, the vapour mass flow rate produced is given by:

$$D_{\mathrm{vap,lab}} = \frac{P_{\mathrm{m}}}{L_{\mathrm{vap,w}}}$$

The latter assumption, neglecting all the heat losses (e.g. radiation at the surface of water, conduction through the water container walls) occurring at the water container level, is supported by the fact that it leads to an overestimation of the required steam superficial speed. Hence, it is ensured that the working point is further away from the lower boundary of superficial speed, for which the extraction of part of the content of the plants in essential oil is compromised. The required steam superficial speed can now be computed, using the following formula, where $d_{t,lab}$ is the inner diameter of the plants tank of the laboratory extraction unit (known value):

$$V_{\mathrm{vap}} = \frac{D_{\mathrm{vap,lab}}}{\rho_{\mathrm{w,vap}} \frac{\pi}{4} {d_{\mathrm{t,lab}}}^2}$$

Moreover, Breyer provides estimations of required extraction times, determined by observing the evolution of the essential oil flow rate at the exit of the extraction unit [6]. This allows determining the mass of water required to perform the extraction and to be placed inside the water container at the beginning of the extraction, as a function of the diameter of the plants tank on site ($d_{\mathrm{t,site}}$):

$$M_{\mathrm{w}} = V_{\mathrm{vap}} \frac{\pi}{4} {d_{\mathrm{t,site}}}^2 \rho_{\mathrm{w,vap}} t_{\mathrm{ext}} \tag{3.3}$$

[6] This small scale extraction unit is entirely made out of glass. The water container is a glass spherical tank, directly placed on a diffuse heating source. The plants tank is a cylinder of 10cm diameter.

3.2.4.2 Solar Concentrator

The solar concentrator is modelled as a parabolic trough, because its construction seems easier than the construction of a parabolic dish, when the means are limited - this was indeed already assessed upon the construction of the existing extraction unit, built on the same site. The parabolic trough is meant to be fully steerable, i.e. it receives the beam component of sun radiation normally at every moment of the day. The assumption is thus made that the parabola is always properly oriented with respect to the sun. Two types of solar concentrators are studied in this section: first mirrors and then an aluminium sheet. The ultimate objective of this section is to evaluate the **overall efficiency of the parabola** η. The latest must take the following phenomena into account:

- a fraction of solar energy is absorbed by the parabola, the rest being reflected. This phenomenon is characterised by the hemispherical reflectance, sometimes simply called **reflectance** here below. The value of this parameter can drop drastically if dirt covers the reflective surface.
- part of the reflected energy does not reach the collector, in a proportion depending on the reflecting surface specularity[7] and manufacturing imperfections (e.g. non perfect parabolic profile). In this work, these effects are referred to as **concentrating efficiency**.

In the scope of this work, it was chosen not to include the influence of the shadow of the solar collector projected on the parabola in the overall efficiency. First, this constitute a more independent way of modelling the parabola with respect to its environment, allowing for an easier adaptation of the model to different collector configurations, and most of all allowing for the sizing of the parabola even if the solar collector dimensions are not known. Second, this choice is partly compensated by the fact that the solar radiation directly reaching the solar collector is not taken into account in its modelling (see section 3.2.4.3). This means that the global model considers that the solar collector receives radiation concentrated by the entire surface of the parabola and nothing directly from the sun. This choice is supported by the fact that the shadow of the collector projected on the parabola is about the same surface as the surface of the collector intercepting the direct solar radiation (the shadow is slightly larger). However, the combination of those two modelling choices underestimates the flux received by the collector, as the direct solar component is also multiplied by the reflectivity of the parabola and its geometrical/mechanical factor. Hence, the global model leads to a small overestimation of the needed parabola surface[8], which ensures that the resulting steam flow rate is a little more than sufficient. To conclude, upon the construction of the solar parabola on site, its surface (projected normally with respect to its focal axis) is simply the result of the sizing computations.

Finally, it is worth noting that the quantity of reflected radiation caught by the solar collector normally depends on its size. Indeed, if the parabolic profile has flaws, some of the reflected light will be deviated from the focal point. The relative importance of this deviation with respect to the size of the collector is however taken into account in the estimation of the concentrating factor.

[7]The specularity of a material refers to the smoothness of its surface. The reflected radiation is split between the main specular reflected radiation and a small part of scattered radiation. The scattered radiation is a diffuse radiation, constituting an additional loss. If a material can be shaped into a perfectly smooth surface, its specular reflectance is equal to the hemispherical reflectance [17].

[8]numeric example : if the projected collector shadow is 15% of the surface of the parabola, if the parabola reflectivity is 80% and its concentrating efficiency is 90%, then the actual received flux by the collector is 85%*80%*90%+15%=76.2% of the total incident flux corresponding to the entire parabola surface. On the other hand, the flux received by the collector according to the model would be 100%*80%*90%=72% of the total incident flux corresponding to the entire parabola surface. This confirms the slight overestimation of the required parabola surface.

3.2.4.2.1 Mirrors Mirrors are characterised by a reflector layer covered with a transparent layer, which role is to protect the reflector from weathering and other wear, allowing to maintain the mirror optical properties. The most common mirrors are made out of a thin layer of silver bonded to a protective layer of glass [17]. As they are probably the most available on site, this section focusses on this kind of mirrors.

- **Reflectivity** The hemispherical reflectance of silver is 98% [17]. However, the protective glass layer absorbs as well, at a rate depending on its quality (composition and presence of impurities) and thickness. Therefore, the reflectance of silver-glass mirrors can vary between 82 and 97%.
- **Concentrating efficiency** First, the specularity of silver-glass is very high, and can even reach 100% [17]. On the other hand, the parabolic profile quality, the ability of the mirrors to stick to the profile, the spacing between mirror pieces depend a lot on manufacturing techniques and design choices (such as the drawing and cutting of the profile, the materials and tools used and the size of the mirror pieces). In this first analysis, it is considered that if the profile is correctly made, the other factors can easily be controlled, allowing for a good concentrating efficiency. Therefore, prior to sizing estimations take into account a concentrating efficiency of 95%.
- **Overall efficiency (η)** The overall efficiency is given by the product of the reflectance with the concentrating efficiency. The lower value of the overall efficiency is thus 82%*95% = 78%.

3.2.4.2.2 Aluminium Sheet Polished aluminium sheets for solar reflection applications are usually protected by a thin anodised[9] film, in order to protect the reflector from weathering and other potential damages.

- **Reflectivity** The hemispherical reflectance of aluminium is 92% [17]. The application of the protective film makes it drop down to 85 to 87%.
- **Concentrating efficiency** Although aluminium reflectors are highly polished in order to improve their specularity, small default and scratches tend to remain. Moreover, the addition of an anodised film increases the scattering phenomenon, which gives specular reflectance values 5 to 15% below the hemispherical reflectance [26]. On the other hand, if a profile of good quality is made, the ability of the aluminium sheet to stick to it depends largely on the technique used to attach them together. The concentrating efficiency can thus vary much. Prior to sizing estimations take into account a concentrating efficiency of 85%.
- **Overall efficiency (η)** Combining reflectance and concentrating efficiency, the lower value of the overall efficiency is 72%.

3.2.4.2.3 Equilibrium Surface Temperature of a Fully Insulated Aluminium Sheet The goal of this section is to implement a model of the parabola allowing to assess the surface temperature of the parabolic concentrator using an aluminium sheet as reflective surface, when it is exposed to solar radiation and has reached equilibrium. In the case studied, the lower surface of the aluminium sheet (index Al) is fully insulated by a thick layer of insulating

[9]Anodising a sheet of aluminium consists in applying a surface treatment that causes the natural layer of aluminium oxide present at the surface of the sheet to thicken, in order to improve the aluminium corrosion properties.

material (index i). To this configuration would correspond the warmest aluminium upper surface temperature, and simplified equations can be used, by assuming that the lower surface temperature of the insulation is equal to the atmospheric temperature, i.e. by neglecting the convective heat losses below the parabola. The following system of equations allows determining T_{p}:

$$\begin{cases} a_{\mathrm{Al}}F = h_{\mathrm{conv}}\left(T_{\mathrm{p}} - T_{\mathrm{atm}}\right) + \varepsilon_{\mathrm{Al}}\sigma\left({T_{\mathrm{p}}}^4 - {T_{sky}}^4\right) + \frac{k_{\mathrm{Al}}}{e_{\mathrm{Al}}}\left(T_{\mathrm{p}} - T_{\mathrm{i}}\right) \\ \frac{k_{\mathrm{Al}}}{e_{\mathrm{Al}}}\left(T_{\mathrm{p}} - T_{\mathrm{i}}\right) = \frac{k_{\mathrm{i}}}{e_{\mathrm{i}}}\left(T_{\mathrm{i}} - T_{\mathrm{b}}\right) \end{cases} \tag{3.4}$$

with T_i the surface temperature at the interface between insulation and aluminium sheet and T_b the surface temperature at the bottom of the insulation.
The parabolic surface is assimilated to a flat plate, and the following Nusselt correlation for the natural convection coefficient was used [8]:

$$\mathrm{Nu}_{\mathrm{L_p}} = 0.54{\mathrm{Ra}_{\mathrm{L_p}}}^{1/4} \tag{3.5}$$

3.2.4.3 Solar Collector

The collector is a horizontal half cylinder of length equal to the length of the parabola, made out of a conductive material (index m for all thermal properties notations) and surrounded by a glass greenhouse (index g for all thermal properties notations), allowing reducing the convection heat losses. The collector geometry corresponds to the geometry of the already existing extraction unit. A transversal cut of this geometry is shown on figure 3.6, together with the notations used for surface temperatures and dimensions. The minimal dimensions of the water container can easily be deduced from the estimated water mass required for the entire extraction (determined thanks to equation 3.3). Indeed, if the common length L_{p} of the water container and the parabola is fixed, the inner radius of the water container r_1 is derived from the water container surface, obtained by simply dividing the required water volume by L_p. In practice, a safety factor should be taken into account, by considering for example twice the required volume of water in the computations. Finally, it is worth noting that here below, the notation S_{i} holds for $(\pi r_{\mathrm{i}} + 2r_{\mathrm{i}})L_{\mathrm{p}}$, with $i = 1, 2, 3, 4$.
Modelling the heat losses occurring at the solar collector level allows **determining the required parabola surface S_{p} to produce the needed steam superficial speed**, for a given plants tank diameter.

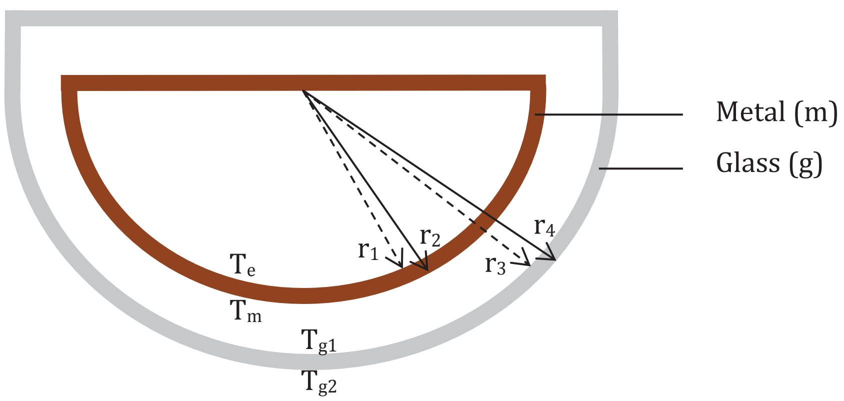

Figure 3.6: Transversal cut of the solar collector configuration and introduction of the notations

3.2.4.3.1 Modelling Assumptions and Considerations

- The whole cylindrical part receives the concentrated radiation reflected by the entire parabolic surface
- There is no contribution of the direct solar heat flux, as mentioned in section 3.2.4.2.
- The surface temperatures are homogeneous along the corresponding surface.
- Regarding the radiative heat fluxes, it is assumed that the inner surface of glass only emits towards the metallic central part (and not towards itself). This assumption is correct as long as the spacing between the greenhouse and the water container is small enough.
- The radiative heat flux received by the glass envelope from its external environment is supposed to be fully emitted by the sky with temperature T_{sky}. Actually, part of the radiative heat flux is emitted by the parabola, having a warmer surface temperature than the sky (obtained by solving system eqParabolaSurfaceTemp). This assumption leads to a slight overestimation of the required parabola surface, as the radiative heat flux received is slightly underestimated[10].
- All the solar flux passing through the glass is absorbed by the water container (no reflection on the collector). This is justified if the water container is black painted (the absorptivity of black paint can reach values up to 0.99 [30]).
- In steady-state, the inner metallic wall temperature, T_e, is equal to the temperature of boiling water at atmospheric pressure, i.e. 100°C.
- During the heating phase, the inner metallic wall temperature T_e is also considered to be equal to the water temperature. Indeed, the temperature evolution of water is sufficiently slow to neglect the effect of a free convection phenomenon within the fluid. The fluid is supposed to be at all time in thermal equilibrium.
- The influence of wind is not taken into account. This means that only the pure natural convection of air is considered along the outer walls.
- The effect of natural convection of air in the enclosure between the solar collector and the greenhouse glass is assessed by computing an effective conductivity coefficient. The correlation for this coefficient is presented in paragraph 3.2.4.3.3 and is valid for concentric cylinders (no correlation was found that matches the solar collector configuration perfectly).

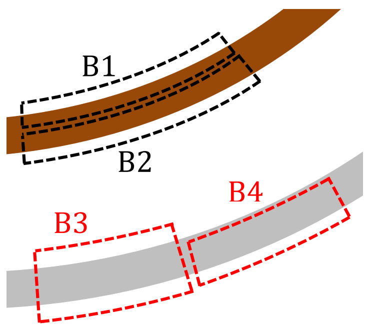

Figure 3.7: Control volumes for the heat balances on the solar collector

[10]The influence of this assumption was checked by doing the computations once with the actual sky temperature, and then replacing it by the equilibrium parabola surface temperature. It lead to only about 2% variation of the required parabola surface.

3.2.4.3.2 Heat Balances Computing the heat balance on each of the control volumes of figure 3.7 allows formulating a system of four equations and four unknowns to solve. In the case of the steady-state case, the four unknowns are S_{p}, T_{m}, $T_{\mathrm{v_1}}$ and $T_{\mathrm{v_2}}$. In the case of the heating phase, once S_{p} is known, the four unknowns at each moment are T_{w}, T_{m}, $T_{\mathrm{v_1}}$ and $T_{\mathrm{v_2}}$.

3.2.4.3.2.1 Balance 1 (B1) Knowing the plants tank diameter on site and the required steam superficial speed, the following equation describes the heat balance on control volume B1 (see figure 3.7) **in steady-state**:

$$k_{\mathrm{m}}\left(T_{\mathrm{m}}-T_{\mathrm{e}}\right)\left(\frac{\pi L_{\mathrm{p}}}{ln\left(r_2/r_1\right)}+\frac{2L_{\mathrm{p}}r_1}{\left(r_2-r_1\right)}\right)=L_{\mathrm{vap,w}}V_{\mathrm{vap}}\frac{\pi}{4}{d_{\mathrm{t,site}}}^2\rho_{\mathrm{w,vap}} \tag{3.6}$$

This expresses the equality between heat fluxes entering (conduction heat flux through the metallic wall) and leaving (heat absorbed by boiling water evaporating at a given mass flow rate) the control volume. The surface considered for the control volume is the surface at which the heat exchange takes place, i.e. the interface metal/fluid.

During the **heating phase**, the following equation holds true:

$$k_{\mathrm{m}}\left(T_{\mathrm{m}}\left(t\right)-T_{\mathrm{e}}\left(t\right)\right)\left(\frac{\pi L_{\mathrm{p}}}{ln\left(r_2/r_1\right)}+\frac{2L_{\mathrm{p}}r_1}{\left(r_2-r_1\right)}\right)=M_{\mathrm{w}}C_{\mathrm{p,w}}\frac{\partial T_{\mathrm{w}}}{\partial t} \tag{3.7}$$

3.2.4.3.2.2 Balance 2 (B2) The following equation describes the heat balance on control volume B2 (see figure 3.7):

$$\begin{aligned}\left(1-a_{\mathrm{g}}\right)F\eta S_{\mathrm{p}}=k_{\mathrm{m}}\left(T_{\mathrm{m}}-T_{\mathrm{e}}\right)\left(\frac{\pi L_{\mathrm{p}}}{ln\left(r_2/r_1\right)}+\frac{2L_{\mathrm{p}}r_1}{\left(r_2-r_1\right)}\right)+\sigma\frac{{T_{\mathrm{m}}}^4-{T_{\mathrm{v1}}}^4}{\frac{1}{\varepsilon_{\mathrm{m}}}+\frac{S_2}{S_3}\frac{1-\varepsilon_{\mathrm{g}}}{\varepsilon_{\mathrm{g}}}}S_2\\+k_{\mathrm{air,eff}}\left(T_{\mathrm{m}}-T_{\mathrm{v1}}\right)\left(\frac{\pi L_{\mathrm{p}}}{ln\left(r_3/r_2\right)}+\frac{2L_{\mathrm{p}}r_2}{\left(r_3-r_2\right)}\right)\end{aligned} \tag{3.8}$$

This balance is valid during the condensing phase as well as during the heating phase, but the latest is characterised by time dependent temperatures instead of steady-state. The time dependency is however not written to lighten the document. This remark holds true for balances 3 and 4 as well. Equation 3.8 expresses the equality between heat fluxes entering (part of solar radiation reflected by the parabola that passes through the greenhouse glass, radiative flux emitted by the glass inner wall towards the water container) and leaving (conductive flux in the metallic wall, radiative flux emitted by the metallic wall towards glass, conductive flux through the air layer) the control volume. The expression of the effective thermal conductivity of the air gap, $k_{\mathrm{air,eff}}$ is presented in paragraph 3.2.4.3.3.
It is worth noting that the part of solar radiation able to reach the metallic wall depends on the clarity of the glass, i.e. on the potential presence of dirt covering it.

3.2.4.3.2.3 Balance 3 (B3) The following equation describes the heat balance on control volume B3 (see fig 3.7):

$$\begin{aligned}\sigma\frac{{T_{\mathrm{m}}}^4-{T_{\mathrm{v1}}}^4}{\frac{1}{\varepsilon_{\mathrm{m}}}+\frac{S_2}{S_3}\frac{1-\varepsilon_{\mathrm{g}}}{\varepsilon_{\mathrm{g}}}}S_2+a_{\mathrm{g}}F\eta S_{\mathrm{p}}+k_{\mathrm{air,eff}}\left(T_{\mathrm{m}}-T_{\mathrm{v1}}\right)\left(\frac{\pi L_p}{ln\left(r_3/r_2\right)}+\frac{2L_pr_3}{\left(r_3-r_2\right)}\right)\\=\varepsilon_{\mathrm{g}}\sigma\left({T_{\mathrm{v2}}}^4-{T_{\mathrm{sky}}}^4\right)S_4+h_{\mathrm{conv}}\left(T_{\mathrm{v2}}-T_{\mathrm{atm}}\right)S_4\end{aligned} \tag{3.9}$$

This expresses the equality between heat fluxes entering (part of solar radiation reflected by the parabola that is absorbed by the glass, radiative flux emitted by the metallic wall towards glass, conductive flux through the air layer, radiative flux emitted by the atmosphere) and leaving (radiative flux emitted by the outer glass wall towards the atmosphere, natural convection flux of air at the outer glass wall, radiative flux emitted by the glass inner wall towards the water container) the control volume. The natural convection coefficient h_{conv} is determined in paragraph 3.2.4.3.4.

3.2.4.3.2.4 Balance 4 (B4) The following equation describes the heat balance on control volume B4 (see fig 3.7):

$$k_{\mathrm{g}}\left(T_{\mathrm{v1}}-T_{\mathrm{v2}}\right)\left(\frac{\pi L_{\mathrm{p}}}{ln\left(r_4/r_3\right)}+\frac{2L_{\mathrm{p}}r_3}{\left(r_4-r_3\right)}\right)+a_{\mathrm{g}}F\eta S_{\mathrm{p}}=\varepsilon_{\mathrm{g}}\sigma\left({T_{\mathrm{v2}}}^4-{T_{\mathrm{sky}}}^4\right)S_4 \\ +h_{\mathrm{conv}}\left(T_{\mathrm{v2}}-T_{\mathrm{atm}}\right)S_4 \tag{3.10}$$

This expresses the equality between heat fluxes entering (part of solar radiation reflected by the parabola that is absorbed by the glass, conductive flux through the glass wall, radiative flux emitted by the atmosphere) and leaving (radiative flux emitted by the outer glass wall towards the atmosphere, natural convection flux of air at the outer glass wall) the control volume. The natural convection coefficient h_{conv} is determined in paragraph 3.2.4.3.4.

3.2.4.3.3 Effective Conductivity of Air As there is a difference of temperature between the metallic half-cylinder and the greenhouse glass, a phenomenon of natural convection takes place in the air gap. The following correlation was found in [9] for concentric cylinders with constant wall temperatures (the notations correspond to those of this section):

$$\frac{k_{\mathrm{air,eff}}}{k_{\mathrm{air}}}=0.386\left(\frac{\mathrm{Pr}}{0.861+\mathrm{Pr}}\right)^{1/4}\left(F_{\mathrm{cyl}}\mathrm{Ra}_{\mathrm{L_c}}\right)^{1/4} \tag{3.11}$$

with $L_{\mathrm{c}}=r_3-r_2$ and $F_{\mathrm{cyl}}=\frac{[\ln(r_3/r_2)]^4}{{L_{\mathrm{c}}}^3\left((2r_2)^{-3/5}+(2r_3)^{-3/5}\right)^5}$

3.2.4.3.4 Nusselt Correlation for the External Natural Convection Coefficient The following experimental correlation gives the Nusselt number for natural convection around a horizontal half-cylinder of diameter d_4 with isothermal walls (steady-state case) [11]:

$$\mathrm{Nu}_{\mathrm{d_4}}=0.78\mathrm{Pr}^{0.27}{\mathrm{Gr}_{\mathrm{d_4}}}^{0.2} \tag{3.12}$$

The computation of the Nusselt number allows deducing the value of the natural convection coefficient h_{conv}.

3.2.4.4 Plants Tank

In steady-state, the heat losses through the tank walls cause part of the vapour flow rate to condense, which is therefore not exiting the plants tank and causes a flow-back towards the water container by gravity effect. This results in a decrease of the vapour flow rate between its entrance in the plants tank and its entrance in the condensing unit. The configuration of the plants tank is presented on figure 3.8 with the notations used in this section.

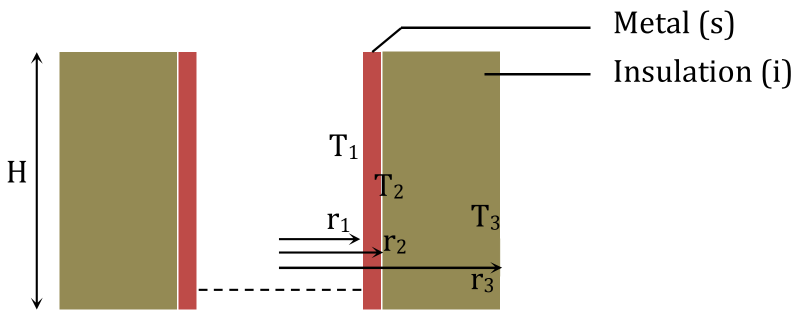

Figure 3.8: Cut of the plants tank and introduction of the notations

3.2.4.4.1 Modelling Assumptions and Considerations

- The oil mass flow rate is neglected with respect to the water mass flow rate.
- The temperature of the inner wall of the tank T_1 is 100°C – no forced convection taken into account inside the tank. This is justified by the fact that the influence of this phenomenon would be negligible in the global heat transfer equation, because the tank is filled with plants and the vapour flow rate is low.
- The absorption of the ambient solar flux is not taken into account, because it is difficult to assess its actual value: the cylinder is vertical, thus the sun orientation plays an important role in the phenomenon. The mass flow rate condensed would thus be less important than the one computed. This must be kept in mind upon addressing the sizing of the condensing unit.
- The outer surface is covered with black plastic, having an emissivity coefficient of 0.94 [1].
- The influence of wind is not taken into account. This means that the pure natural convection of air is considered along the outer walls.

3.2.4.4.2 Heat Balances The heat balances are expressed by the equality between heat fluxes entering and leaving at each interface of the plants tank: interface plants bed/ metal (control volume I1), interface metal/insulation (control volume I2) and interface insulation/atmospheric air (control volume I3) (see figure 3.9).

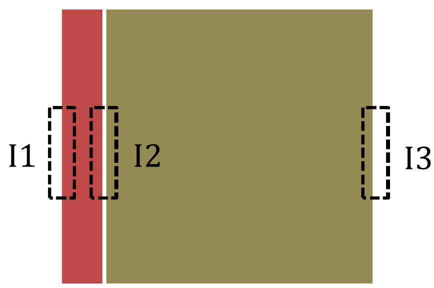

Figure 3.9: Control volumes for the plants tank balances

3.2.4.4.2.1 Interface 1 (I1) The heat loss through the walls of the cylinder causes part of the vapour flow rate to condense, in such a way that the mass flow rate entering the condensing unit D_{condens} is lower than the flow rate entering the plants tank D_{vap}. This is expressed by the following equation:

$$\left(D_{\text{vap}} - D_{\text{condens}}\right) L_{\text{vap,w}} = \frac{k_{\text{s}}}{ln\left(r_2/r_1\right)} \left(T_1 - T_2\right) * 2\pi H \tag{3.13}$$

3.2.4.4.2.2 Interface 2 (I2) The following equation describes the equilibrium between conduction heat fluxes on both sides of the interface:

$$\frac{k_{\text{s}}}{ln\left(r_2/r_1\right)} \left(T_1 - T_2\right) = \frac{k_{\text{i}}}{ln\left(r_3/r_2\right)} \left(T_2 - T_3\right) \tag{3.14}$$

3.2.4.4.2.3 Interface 3 (I3) The following equation describes the equilibrium between the conduction heat flux in the insulation and the convection and radiation heat fluxes at the insulation outer wall:

$$\frac{k_{\text{i}}}{ln\left(r_3/r_2\right)} \left(T_2 - T_3\right) 2\pi H = \left(\varepsilon_{\text{i}}\sigma \left({T_3}^4 - {T_{\text{sky}}}^4\right) + h_{\text{conv}} \left(T_3 - T_{\text{atm}}\right)\right) 2\pi r_3 H \tag{3.15}$$

3.2.4.4.3 Nusselt Correlation for the Natural Convection Coefficient The following equation gives the Nusselt correlation for the natural convection along a vertical cylinder with isothermal walls, with the notations corresponding to those used in this paragraph [10]:

$$\text{Nu}_{\text{H}} = \frac{4}{3}\left(\frac{\frac{7}{5}\text{Ra}_{\text{H}}\text{Pr}}{20 + 21\text{Pr}}\right)^{(1/4)} + \frac{4}{35}(272 + 315\text{Pr})\frac{H}{(64 + 63\text{Pr})2r_3} \tag{3.16}$$

3.2.4.5 Condensing Unit

The condensing unit is a set of pipes linked together and put inside a tank full of water, in a spiral configuration. There are two phases to the cooling process: first, the vapour flow rate is condensed, and then the product is cooled down. The ultimate goal of this section is to **determine the surface of condensing pipes necessary to condense and cool down the distillation products exiting the plants tank** (water and oil under the vapour state). Each small section of pipe is modelled as a horizontal cylinder, whose configuration is presented on figure 3.10 with the notations used in this section.

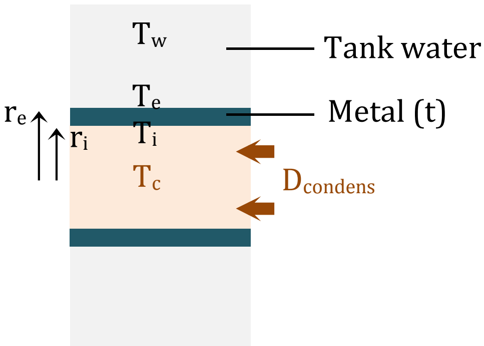

Figure 3.10: Cut of a condensing pipe and introduction of the notations

3.2.4.5.1 Modelling Assumptions and Considerations

- The mass flow rate of oil is neglected with respect to the flow rate of water. Indeed, the volume flow rate of oil is about 3% of the water volume flow rate [6], which corresponds to an even lower mass flow rates ratio.

- The values of the specific heat capacity, the latent heat of vaporisation and the thermal conductivity of water are used for the mixture of water and oil.
- The pipes linking the tank to the condensing unit are not taken into account. This ensures a sufficient sizing of the condensing unit – indeed heat is already exchanged with the atmospheric medium through the walls of those pipes, so that less heat needs to be absorbed by the condensing unit.
- The temperature of water in the condensing tank is uniform and kept down to 50°C. This temperature corresponds to the maximum temperature recommended by Breyer, above which it is difficult to separate the oil from the water phase [6]. The maximum temperature of 50°C is thus a requirement.
- The temperature of the distillation product at the exit of the condensing unit is 60°C.

3.2.4.5.2 Heat Balances

3.2.4.5.2.1 Condensing phase During this phase, it is considered that vapour travels inside the pipes, the surface of which allows for the heat transfer corresponding to the change of phase from vapour to liquid of the vapour flow entering the condensing unit. The internal flow is characterised by the thermal properties of steam.
The type of convection (natural, forced or mixed) occurring inside the pipes is first verified, through the computation of the Richardson number. First, the Reynolds number can easily be computed from the mass flow rate entering the condensing unit and the inner diameter of the pipes, using the following formula:

$$\mathrm{Re}_{d_\mathrm{i}} = \frac{D_\mathrm{condens}}{\rho_\mathrm{w,vap}\pi\frac{{d_\mathrm{i}}^2}{4}}\frac{d_\mathrm{i}}{\nu_\mathrm{w,vap}} \tag{3.17}$$

The Grashof number value can priorly be assessed, considering for example a difference of temperature of 20 degrees between the distillation products and the pipes inner wall temperature. As will be seen in section 3.2.5, the result of those computations shows that the convection inside the pipes during the condensing phase is mostly forced, leading to a forced convection Nusselt correlation (given in paragraph 3.2.4.5.3).

For a given pipes radius r_i, the total length of piping $L_\mathrm{pi,c}$ required for the condensing of the distillate can thus be determined solving the following set of three equations with three unknowns ($L_\mathrm{pi,c}$, T_i and T_e):

$$\begin{cases} D_\mathrm{condens}L_\mathrm{vap,w} = h_\mathrm{fconv}\left(T_\mathrm{c} - T_\mathrm{i}\right)2\pi r_\mathrm{i}L_\mathrm{pi,c} \\ h_\mathrm{fconv}\left(T_\mathrm{c} - T_\mathrm{i}\right)2\pi r_\mathrm{i}L_\mathrm{pi,c} = \frac{k_\mathrm{t}}{ln(r_\mathrm{e}/r_\mathrm{i})}\left(T_\mathrm{i} - T_\mathrm{e}\right)2\pi L_\mathrm{pi,c} \\ \frac{k_\mathrm{t}}{ln(r_\mathrm{e}/r_\mathrm{i})}\left(T_\mathrm{i} - T_\mathrm{e}\right)2\pi L_\mathrm{pi,c} = h_\mathrm{conv}\left(T_\mathrm{e} - T_\mathrm{w}\right)2\pi r_\mathrm{e}L_\mathrm{pi,c} + \varepsilon_\mathrm{t}\sigma\left({T_\mathrm{e}}^4 - {T_\mathrm{w}}^4\right)2\pi r_\mathrm{e}L_\mathrm{pi,c} \end{cases} \tag{3.18}$$

The correlations for the Nusselt numbers allowing to compute the natural convection coefficient occurring at the outer wall of the pipes is also provided in paragraph 3.2.4.5.3.

3.2.4.5.2.2 Cooling phase In the case of the cooling phase, all the fluid thermal properties are the ones of liquid water. In each infinitesimal length of pipe, the temperatures are considered steady, i.e. once steady-state is reached, the walls temperatures in each point of the cooling pipes are constant. Here, the prior computation of the Reynolds and Grashof numbers for the liquid water flowing inside the pipes shows that the flow is laminar and the free convection has a significative influence on the convection heat exchange (see section 3.2.5); the internal convection is thus mixed. This leads to the following system of equations, with $h_{\mathrm{mconv,i}}$ and $h_{\mathrm{conv,e}}$ the convection coefficients for the internal and external heat exchanges respectively:

$$\begin{cases} C_{\mathrm{p,w}} D_{\mathrm{condens}} \frac{\partial T_{\mathrm{c}}}{\partial L} = h_{\mathrm{mconv,i}} \left(T_{\mathrm{c}} - T_{\mathrm{i}}\right) 2\pi r_{\mathrm{i}} \\ h_{\mathrm{conv,i}} \left(T_{\mathrm{c}} - T_{\mathrm{i}}\right) 2\pi r_{\mathrm{i}} L_{\mathrm{pi,co}} = \frac{k_{\mathrm{t}}}{ln(r_{\mathrm{e}}/r_{\mathrm{i}})} \left(T_{\mathrm{i}} - T_{\mathrm{e}}\right) 2\pi L_{\mathrm{pi,co}} \\ \frac{k_{\mathrm{t}}}{ln(r_{\mathrm{e}}/r_{\mathrm{i}})} \left(T_{\mathrm{i}} - T_{\mathrm{e}}\right) 2\pi L_{\mathrm{pi,co}} = h_{\mathrm{conv,e}} \left(T_{\mathrm{e}} - T_{\mathrm{w}}\right) 2\pi r_{\mathrm{e}} L_{\mathrm{pi,co}} + \varepsilon_{\mathrm{t}} \sigma \left({T_{\mathrm{e}}}^4 - {T_{\mathrm{w}}}^4\right) 2\pi r_{\mathrm{e}} L_{\mathrm{pi,co}} \end{cases} \tag{3.19}$$

The Nusselt correlations for mixed and natural convection coefficients are provided in paragraph 3.2.4.5.3.
System 3.19 can be solved by considering a certain number of pipes section of length $\Delta L_{\mathrm{pi,co}}$, in which the internal flow enters at a temperature equal to the temperature it had leaving the previous section. The initial entrance value is the temperature of boiling water (at the transition from condensing phase) and the final exit value is 60°C. The three unknowns for each pipe section are thus the exit temperature of the internal flow $T_{\mathrm{c}}(\mathrm{exit})$, T_{i} and T_{e}.

3.2.4.5.3 Nusselt Correlations

3.2.4.5.3.1 External Natural Convection The Nusselt correlation for natural convection around a horizontal cylinder is $\mathrm{Nu} = C{\mathrm{Ra}_{\mathrm{d_e}}}^n$ with d_{e} the pipes outer diameter and C and n depending on the associated Raleigh number in the following way [8]:

- $\mathrm{Ra}_{\mathrm{d_e}} \leq 10^{-2} : C = 0.675; n = 0.058;$
- $10^{-2} < \mathrm{Ra}_{\mathrm{d_e}} \leq 10^{2} : C = 1; n = 0.148;$
- $10^{2} < \mathrm{Ra}_{\mathrm{d_e}} \leq 10^{4} : C = 0.85; n = 0.188;$
- $10^{4} < \mathrm{Ra}_{\mathrm{d_e}} \leq 10^{7} : C = 0.48; n = 0.25;$
- $10^{7} < \mathrm{Ra}_{\mathrm{d_e}} \leq 10^{12} : C = 0.125; n = 0.333;$

3.2.4.5.3.2 Condensing Phase Internal Convection In order to choose a correlation for forced convection, it is required to first assess the type of flow occurring in the pipes when the distillation product is flowing, with respect to each phase. The flow can be laminar, transition or turbulent.
In the case of laminar flows, the following Nusselt correlation is used, for a constant heat flux flowing through the pipes walls [8]:

$$\mathrm{Nu}_{\mathrm{d_i}} = 4.36 \tag{3.20}$$

Flows with Reynolds numbers superior to the transition value of 2300 present a certain level of turbulence, and in this case the following Nusselt correlation holds true [21]:

$$\mathrm{Nu}_{\mathrm{d_i}} = \frac{(f/8)\left(\mathrm{Re}_{\mathrm{d_i}} - 1000\right)\mathrm{Pr}}{1 + 12.7\sqrt{f/8}\left(\mathrm{Pr}^{2/3} - 1\right)} \tag{3.21}$$

with

$$f = \frac{1}{\left(1.82\log_{10}\mathrm{Re}_{\mathrm{d_i}} - 1.64\right)^2} \tag{3.22}$$

Finally, flows with Reynolds numbers superior to 4000 are fully turbulent and are characterised by the following Nusselt relation [8]:

$$\mathrm{Nu}_{\mathrm{d_i}} = 0.023 {\mathrm{Re}_{\mathrm{d_i}}}^{0.8} \mathrm{Pr}^{0.4} \tag{3.23}$$

3.2.4.5.3.3 Cooling Phase Internal Convection The Nusselt correlation for the convection of a fluid flowing inside a pipe of inner diameter d_i is [24]:

$$\mathrm{Nu}_{\mathrm{d_i}} = 3.18935 \left(\frac{\mathrm{Ra}_{\mathrm{d_i}}}{\mathrm{Re}_{\mathrm{d_i}}} \right)^{0.26352} \tag{3.24}$$

This correlation is valid for laminar flows (verified in the case of the cooling phase, as will be seen in section 3.2.5) and takes into account the effect of the free convection often occurring at low Reynolds number.

3.2.5 Sizing Simulation

The model of the extraction unit established in the previous section was implemented under the form of Matlab codes (available in appendix B). In this section, a simulation is run presenting the results obtained for the main parameters, starting from a set of materials and dimensions for the different parts of the extraction unit. On site, all those materials and dimensions data will have to be adapted to the actual data, function of the availability of the materials and the construction methods.

Site climate conditions
$p_\mathrm{atm} = 1$ [atm]
$T_\mathrm{atm} = 313.15$ [K]
$t = 12$ [h]
$RH = 0.3$ [-]
$T_\mathrm{sky} = 299.05$ [K]
$F = 1000$ [W/m^2]

Predeterminations	
Laboratory	Site arbitrary data
$P_\mathrm{m} = 250$ [W]	$M_\mathrm{p} = 1$ [kg]
$d_\mathrm{t,lab} = 250$ [W]	$t_\mathrm{ext} = 3$ [h]
$V_\mathrm{vap} = 0.024$ [m/s]	Results
	$M_\mathrm{w} = 2.69$ [kg]

1. Solar concentrator	
Reflector material: aluminium	Dimensions
$k_\mathrm{Al} = 200$ [W/(m.K)]	$L_\mathrm{p} = 1.5$ [m]
$a_\mathrm{Al} = 0.15$ [-]	$e_\mathrm{Al} = 0.001$ [m]
$\varepsilon_\mathrm{Al} = 0.09$ [-]	$e_\mathrm{i} = 0.05$ [m]
$\eta = 72$ [%]	Computation results
Insulation material: glass wool	$T_\mathrm{p} = 323.15$ [K]
$k_\mathrm{i} = 0.04$ [W/(m.K)]	$S_\mathrm{p} = 1.05$ [m^2]

2. Solar collector	
Water container: aluminium	Dimensions
$k_{\mathrm{m}} = 200$ [W/(m.K)]	$r_1 = 0.05$ [m]
Black paint	$r_2 = 0.0515$ [m]
$\varepsilon_{\mathrm{m}} = 0.9$ [-]	$r_3 = 0.0715$ [m]
Greenhouse: glass	$r_4 = 0.0765$ [m]
$k_{\mathrm{g}} = 0.7$ [W/(m.K)]	Computation results
$a_{\mathrm{g}} = 0.05$ [-]	$D_{\mathrm{vap}} = 2.49 * 10^{-4}$ [kg/s]
$\varepsilon_{\mathrm{m}} = 0.9$ [-]	
Air gap	
Air thermal properties at 60°C	
$k_{\mathrm{air,eff}} = 0.054$ [W/(m.K)]	

3. Plants tank		
Tank: stainless steel 340	Dimensions	Computation results
$k_{\mathrm{s}} = 17$ [W/(m.K)]	$r_1 = 0.075$ [m]	Percentage of condensed mass flow rate $\simeq 1\%$
Insulation: glass wool	$r_2 = 0.08$ [m]	The loss in mass flow rate is neglected
$k_{\mathrm{i}} = 0.04$ [W/(m.K)]	$r_3 = 0.13$ [m]	
	$H = 0.225$ [m]	

4. Condensing unit			
Materials	Stainless steel 340	Main computation results	
	$k_{\mathrm{t}} = 17$ [W/(m.K)]	$D_{\mathrm{condens}} = 2.49 * 10^{-4}$[kg/s]	
	$\varepsilon_{\mathrm{t}} = 0.85$ [-]	Condensing phase	Cooling phase
Dimensions		$\mathrm{Re}_{\mathrm{d_i}} = 2587$	$\mathrm{Re}_{\mathrm{d_i}} = 58$
$r_{\mathrm{i}} = 0.005$ [m]		$\mathrm{Ri}_{\mathrm{d_i}} = 3 * 10^{-5}$	$\mathrm{Ri}_{\mathrm{d_i}} = 14$
$r_{\mathrm{e}} = 0.006$ [m]		$L_{\mathrm{pi,c}} = 13.15$ [m]	$L_{\mathrm{pi,co}} = 0.28$[m]

3.2.6 Sensitivity Analysis

The main objectives of the sizing of the extractor were presented in section 3.2.3. The goal of this section is to assess the proportion in which these objectives would not be met if some of the parameters of the modelling phase were not estimated correctly or if the climate conditions vary. First, the steam superficial speed variations are analysed as a function of a number of parameters: parabola efficiency, variation of the solar direct flux. The influence of the plants tank diameter on the required parabola surface is also assessed. Second, the variations of the piping length of the condensing unit are studied as a function of the entering flow rate, the pipes inner radius and the temperature of water in the condensing tank. Each study is characterised by the set of parameters presented in section 3.2.5, except for the studied parameters that are varying within the studied range.

3.2.6.1 Superficial Speed of Steam

Figure 3.11 shows that the resulting superficial speed of steam through the plants bed varies linearly when either the parabola efficiency or the direct solar flux vary around the working point of section 3.2.5 (labelled on figure 3.11). A comfortable margin is available in both cases. First, if an error was made upon estimating the parabola efficiency, this error can rise up to 22%

of parabola efficiency before the working point steps out of the boundaries. Moreover, it is most likely that the upper boundary would never be reached, as it corresponds to a very high value of the parabola efficiency (94 %), only achievable with high quality reflective materials that are probably not available on site. On the other hand, the direct solar flux can vary of about 300 W/m^2 around the studied working point before stepping out of the boundaries. Once again, the upper boundary would never be reached, as it corresponds to a very high value of the solar flux density (1300 W/m^2) that occurs only at the hottest time of particular days with very bright sky (according to fields observations made during the author's stay in Ouagadougou).

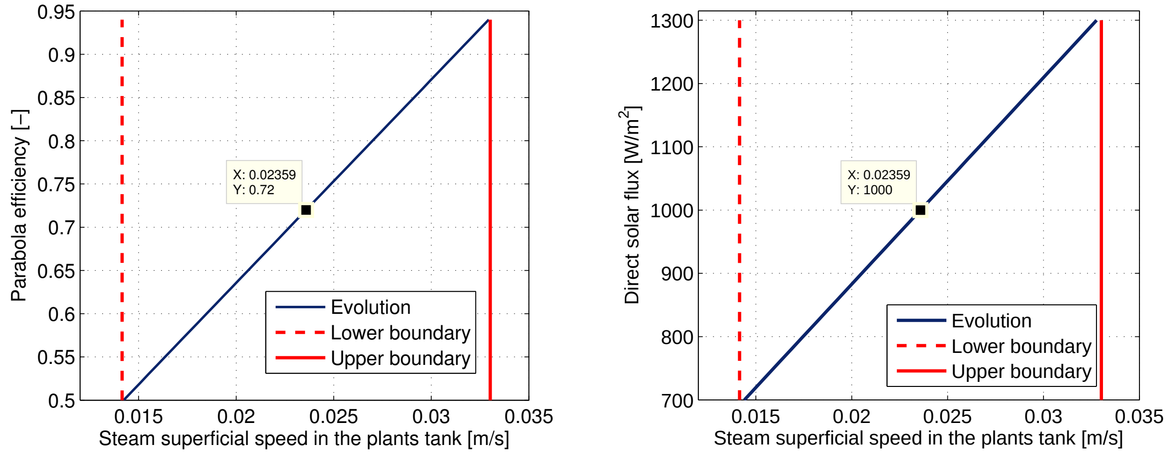

(a) Parabola efficiency

(b) Direct solar flux

Figure 3.11: Evolution of the steam superficial speed as a function of the parabola efficiency and the direct solar flux. The boundaries for the allowable superficial speeds of steam are also plotted.

Figure 3.12 shows the parabolic dependency of the parabola surface required with respect to the plants tank diameter, for the working point defined in section 3.2.5. In order to spare reflective material, expected to constitute a major part of the total costs of the extraction unit, a tank of small diameter and large height is preferred to large diameters tanks, for a given volume of plants to treat.

Figure 3.13 shows the influence of the water container length on the parabola surface required. For a same inner volume (equal to twice the volume of the mass of water required for the extraction), the heat losses are higher if the length of the water container increases, because in that case the heat exchange surface is larger. Upon fixing the dimensions of the extraction unit before its construction, this dependency must be kept in mind in order to limit the parabola surface required.
Figure 3.13 also shows the influence of the presence of the glass greenhouse around the water container. The red curve, obtained by adapting the balances of section 3.2.4.3, corresponds to the parabola surface that would be required if the glass greenhouse were not built. It can be observed that the glass envelope allows saving about 10% of parabola surface, this percentage increasing with the length of the water container. This shows the ability of the glass greenhouse to limit the heat losses of the system, by protecting the hot water container from air natural convection. The fact that the greenhouse influence is higher when the water container length increases is due to the fact that this increase in length is accompanied by a decrease in diameter, for the same inner volume, and that the free convection heat losses depend on the water container diameter with the power of -0.4.

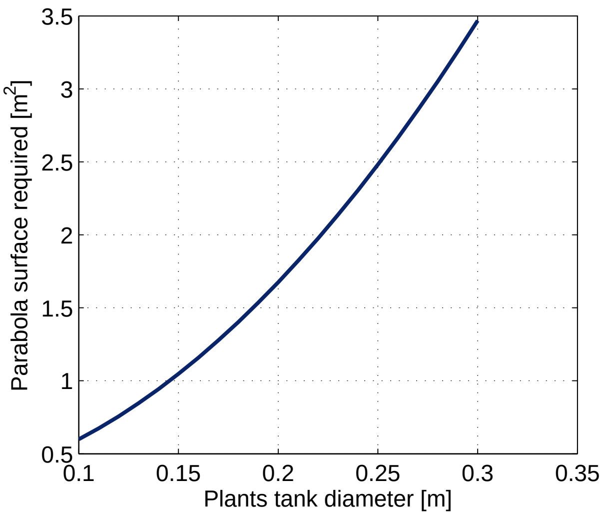

Figure 3.12: Parabola surface required as a function of the plants tank diameter

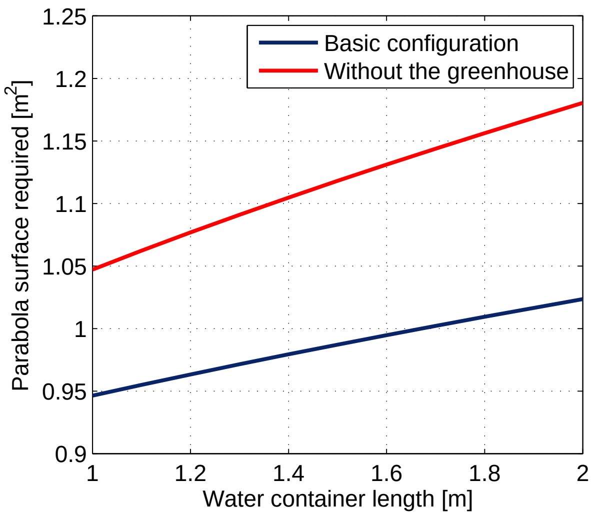

Figure 3.13: Parabola surface required as a function of the water container length, for the same volume - Influence of the presence of the glass greenhouse

3.2.6.2 Condensing Pipes Length

In this section, the influence of the flow rate of the distillation products on the total length of pipes required to ensure their condensing and cooling is studied, for the working point defined in section 3.2.5. For a better visualisation of the results, the flow rate of the distillation products is represented by the plants tank diameter, as those two variables are directly related, for a same steam superficial speed occurring in the plants bed.

During the condensing phase, the flow of the distillation products inside the pipes is always characterised by a Richardson number a lot smaller than 1 (see figure 3.16). Therefore, forced convection is always dominating during the condensing phase. On the other hand, figures 3.14 and 3.15 show the important influence of the type of flow during the condensing phase. Indeed, the switches from laminar to transition and from transition to turbulent allow both reducing the length of pipes required. In the case of the switch from laminar to transition, this reduction is drastic, allowing saving more than 50% of pipes length. Therefore, during the sizing of the extraction unit, it is very important that the flow type in the pipes during the condensing phase is at least transition, or turbulent. This can be achieved by controlling the plants tank diameter on the one hand, but also the inner diameter of the condensing pipes.

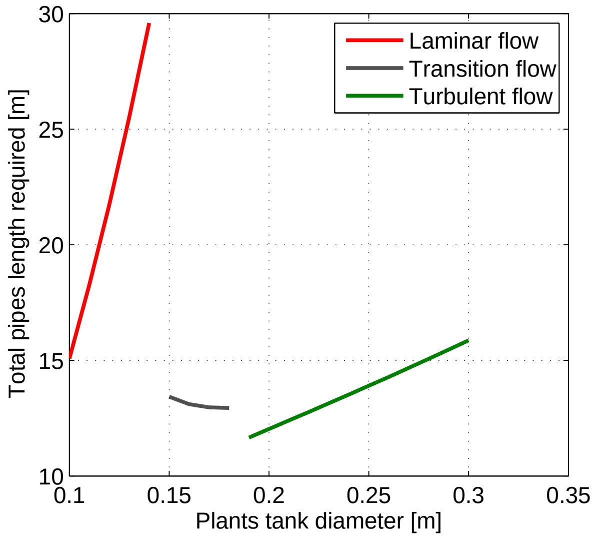

Figure 3.14: Total length of pipes required for the condensing and cooling of the distillation products as a function of the plants tank diameter - Influence of the type of flow during the condensing phase

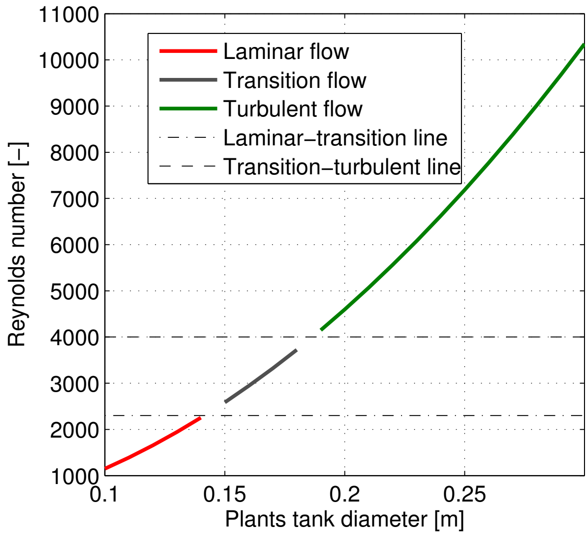

Figure 3.15: Evolution of the Reynolds number characterising the flow of the distillation products during the condensing phase (vapour) as a function of the plants tank diameter

Finally, as shown on figures 3.17 and 3.18, the liquid flow of the cooling phase is always laminar and characterised by an important part of natural convection in the internal heat exchanges, which justifies the use of the correlation presented in paragraph 3.2.4.5.3.3.

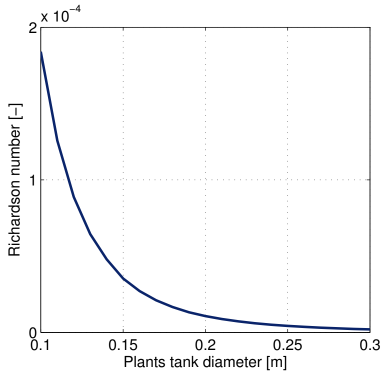

Figure 3.16: $\mathrm{Ri}_{\mathrm{d_i}}$ as a function of $d_{\mathrm{t,site}}$ during the condensing (vapour) phase

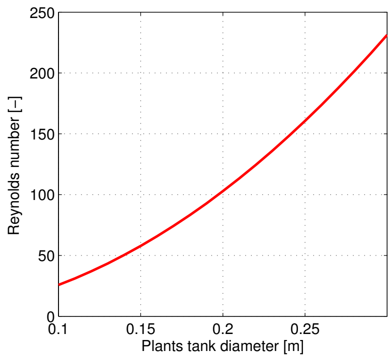

Figure 3.17: $\mathrm{Re}_{\mathrm{d_i}}$ as a function of $d_{\mathrm{t,site}}$ during the cooling (liquid) phase

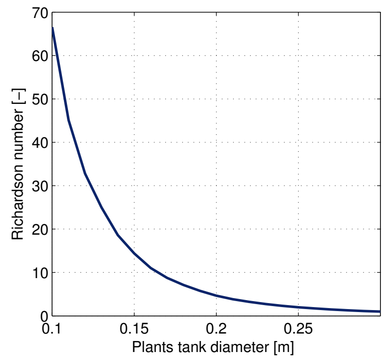

Figure 3.18: $\mathrm{Ri}_{\mathrm{d_i}}$ as a function of $d_{\mathrm{t,site}}$ during the cooling (liquid) phase

The influence of the temperature of the water of the condensing tank is now analysed. Figure 3.19 shows that reducing the water temperature of 25 K from the working point of section 3.2.5 allows reducing the total length of pipes required by approximately 35%. This shows the great advantage that a cool circulating flow of water would constitute, instead of stagnant water. Unfortunately, this is probably not feasible on site, because of the outdoor usage probably far away from any water source and the costs in water if it is just running through the tank and then wasted, or the costs in pumping material if a closed circuit is conceived.

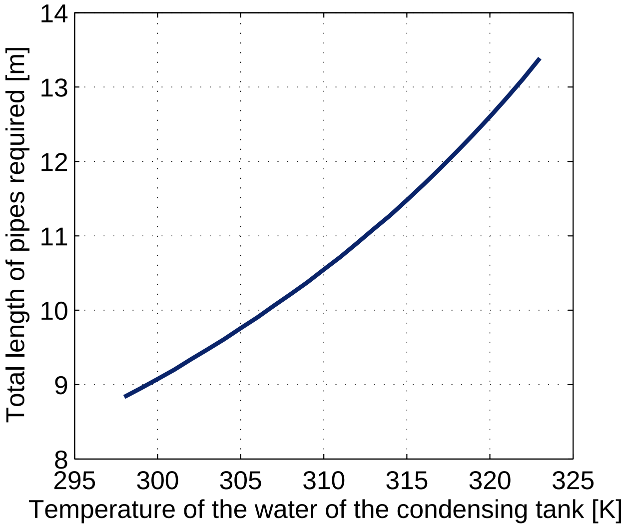

Figure 3.19: Influence of the temperature of the water of the condensing tank on the total length of pipes required

3.2.7 Conclusion

The modelling and analysis of the different subsystems of the extraction unit allows drawing several guidelines for the construction of the extraction unit on site, whose climate conditions should be determined during the first days following the arrival in Ouagadougou (available solar flux during the duration of an extraction, temperature, relative humidity, etc.).
It is recommended to first buy or initiate the manufacturing of the plants tank. Indeed, the latter highly influences the requirements in terms of reflective surface. Reducing the plants tank allows a reduction of the reflective area. The tank should however remain large enough to contain as many plants as required.
Then, the water collector can be sized, knowing that reducing the cylinder length allows reducing the heat losses. This must however be related to the parabola surface required, to avoid the need for manufacturing a parabola a lot wider than long, for which the concentrating losses due to manufacturing profile flaws are expected to be more important.
Once its length is fixed, the parabola can be constructed.
In the mean time, condensing pipes with a diameter allowing for the circulation of a transition or turbulent flow of the incoming vapour flow rate can be purchased.

Chapter 4

Construction of a new Extraction Unit on Site and Testing

4.1 Construction Objectives

In the framework of the inter-university cooperation linking the Université libre de Bruxelles (ULB) and the Université de Ouagadougou (UO), collaborative projects were undertaken since 2009, some of them regarding the extraction of essential oils. In 2009, an extraction unit was built, with the involvement of ULB Master students, UO professors and the workers of the Atelier Central de Maintenance of the UO. This unit, shown on figure 4.1 and analysed in section 4.2, was used as a didactic prototype by local and Belgian students and PhDs. The studies performed showed that its performances are globally insufficient, producing oils of bad quality while the extraction duration is too long. The construction of a new extraction unit aims at obtaining a more efficient prototype, on the basis of the materials selection and rational sizing performed in chapter 3. In order to manage the construction of the new unit, the author left for a six weeks stay in Ouagadougou, from February 16 to March 29 2013, during the dry season.

Figure 4.1: Existing unit at the Université de Ouagadougou

The primary requirements for the new extraction unit are the following:

- it should be smaller in size and most of all easier to manipulate than the existing unit.
- it should be able to process 1 kg of plants leaves.
- it is aimed to be used during the dry season, at the rate of one extraction per day.
- learning should be made from the existing extraction unit in order to reuse its positive features and avoid the negative ones.

- local construction materials should be used.
- the construction should be carried out with the full and only cooperation of the workers of the ACM. Therefore the design must suit the available manufacturing techniques. Those are reviewed in section 4.7.
- each decision regarding the construction is discussed with the head of the ACM, Adama Ouédraogo, in order to make use of his technical expertise.

4.2 Analysis of the Existing Extraction Unit

In this section, each part of the existing extraction unit as categorised in section 1.3.2 is analysed on the basis of a thorough observation on site.

4.2.1 Extraction System

4.2.1.1 Plants Tank

Figure 4.2 shows different views of the plants tank of the existing extraction unit. It is made out of an aluminium cylindrical tank, obtained by modifying a pressure cooker. The external walls, bottom and cover are wrapped with glass wool, surrounded with black plastic. A hole was punched in the bottom of the plants tank in order to allow steam impregnating the plants bed, and a galvanized steel connector was welded in the hole. A second hole was pierced in the cover to allow for the evacuation of the distillation products towards the condensing tank (see figure 4.2c), and a copper connector was welded in the hole. A flat seal was applied along the cover perimeter to insure the tightness of the subsystem (see figure 4.2c). The vapour homogenisation system is an aluminium plate pierced with many small holes, that is placed in the bottom of the tank (see figure 4.2b). It also prevents the plants leaves from dropping inside the water container situated just bellow.
The inside of the tank is found dirty, with dried traces of plants substances that ran along the walls and on the vapour homogenising grid. However, no clear sign of corrosion was found.

(a) External view (b) Internal view (c) Flat seal inside the cover

Figure 4.2: Pictures of the plants tank of the existing extraction unit

Table 4.1 presents the dimensions of the plants tank subsystem.

Tank	$d_{\mathrm{t,site}} = 0.32$ [m]
	$e_{\mathrm{t,site}} = 0.004$ [m] (estimated)
Insulation	$e_{\mathrm{i}} = 0.02$ [m] (estimated mean value)

Table 4.1: Dimensions of the plants tank subsystem of the existing extraction unit

4.2.1.2 Condensing Unit

The pipework of the condensing unit is made out of seven stainless steel hoses of 42 cm each (figure 4.3a). Three of them ensure the connection between the plants tank and the four other spiral bended pipes immersed in the condensing tank. The material of the pipes connectors is unknown, but its colour and the absence of oxidation traces indicate brass. The evacuation of the distillate from the condensing unit is ensured by a copper tap. The tightness of the whole subsystem is ensured by red cardboard gaskets of adapted sizes (see figure 4.3b).
The stainless steel hoses and their connectors appear perfectly neat and unaltered. No trace of corrosion is observable. However, the copper tap is heavily oxidised (it shows a black colour). Also, the gaskets seam to show localised fading, which might indicate that some pigments of the gaskets dissolved in the distillation products.

(a) Piping, tap and gaskets

(b) Zoom on gaskets

Figure 4.3: Pictures of the pipework of the condensing unit, with accessories

Table 4.2 presents the dimensions of the hoses.

Hoses	$r_{\mathrm{pi}} = 0.006$ [m]
	$e_{\mathrm{pi}} = 0.001$ [m] (estimated)

Table 4.2: Dimensions of the stainless steel hoses of the existing unit

The condensing tank is cylinder of about 50 cm diameter and 60 cm height, made out of a 2 mm low carbon steel sheet. The anti-rust paint applied during the studies of March 2012 by Breyer [6] is mostly worn off, such that rust is covering the inner walls of the condensing tank.

4.2.1.3 Separator

Figure 4.4 shows the syphon system conceived to allow separating the essential oils from the distillation water. As its density is lower than the density of water, essential oil floats at the surface of water. The syphon system allows evacuating the water through the bottom of the separator, while the essential oil stays in the separator. It is collected at the end of the extraction.

Figure 4.4: Separator

4.2.2 Vapour Generation System

4.2.2.1 Solar Concentrator

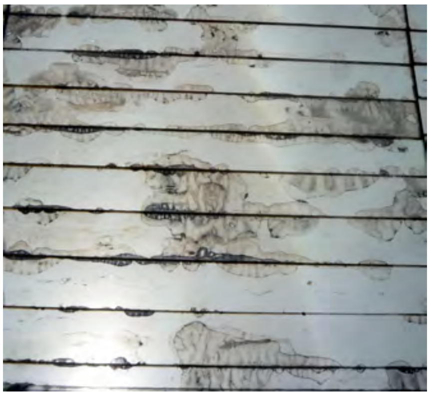

Figure 4.5: Corrosion of the reflecting surface of the mirrors of the existing extraction unit

The reflective surface of the existing parabola is composed of glass mirror laths of about 5 x 50 cm, that are glued on the parabolic profile. As far as it could be observed, all the specular reflected solar flux is reaching the collector, this corresponding to a high concentrating efficiency. However, some chemical reaction between the glue and the mirror reflector seemed to corrode the latter on large regions of the parabola (figure 4.6). This potentially decreased the reflective efficiency, in a proportion that is a priori unknown. Also some glass fragments are missing as a result of wear.
The parabolic profile was shaped in wood, constituting the whole supporting structure of the solar concentrator.

4.2.2.2 Solar Collector

Figure 4.6: Half-cylindrical solar collector

The solar collector is made out of a half-cylindrical water container, shaped from a low carbon steel sheet, covered with black mat paint. The top of the half-cylinder is inclined symmetrically with respect to the exit hole, to allow for the natural circulation of steam towards it. On the exit hole a connector is threaded allowing the fixation of the plants tank.
A greenhouse surrounds the water collector. It is made out of multiple glass laths of about 5 cm width that are arranged along a low carbon steel half-cylindrical profile. Larger pieces of glass are used for the top of the greenhouse, which is flat. The glass pieces are joined together with silicon.
It can be observed that, with time, red sand from the ground accumulated inside the greenhouse through the small openings remaining despite of the silicon joints. Therefore, the inner glass wall is dirty, but can only be washed if the silicon joining the top to the half-cylindrical part is removed first.

Table 4.3 presents the dimensions of the solar collector, with the notations used in section 3.2.4.3.

Water container	$r_1 = 0.15$ [m] (estimated)
	$e_\mathrm{m} = 0.0015$ [m]
Air	$e_\mathrm{a} = 0.05$ [m] (estimated)
Greenhouse	$e_\mathrm{g} = 0.005$ [m]
Length	$L_\mathrm{p} = 2.5$ [m]

Table 4.3: Dimensions of the solar collector of the existing unit

4.3 The Atelier Central de Maintenance

The Atelier Central de Maintenance (ACM) of the Université de Ouagadougou (UO) aims at providing the required maintenance to any structure of the campus of the UO, in a various number of fields (furniture, transport vehicles, cooling systems, electronics, etc.). About fifteen workers specialised in one or several disciplines are working under the leadership of Adama Ouédraogo, head of the department. The means are rather limited, but the experience and knowledge of the team often allows finding creative solutions.
Here bellow the different construction workshops available at the ACM are reviewed:

- **Carpentry** The workshop includes manual saws, circular saws, drills and squares.
- **Metal work**
  - **Joining** The workshop includes gas welding with filler metal (see figure 4.7). Brazing tools are not available but easily accessible at an independent contractor's workshop.
  - **Cutting** The workshop includes an abrasive saw, a bench shear allowing to cut metal sheets easily, and a drilling machine.
  - **Bending** A roll bending machine is available.

Figure 4.7: Gas welding workshop

4.4 Design Focus Points, Alternatives, Choices and Construction

4.4.1 General

Upon conceiving the new extraction unit, several general design focus points should be considered:

- Each part should fulfil its primary functions.
- The removable parts should be easy to mount and dismount.
- The maintenance of each part should be easy to do.
- The moveable parts should be easy to handle during use and maintenance.
- The materials should be bought locally, while being consistent with the materials selection performed in section 3.1.

- Regarding the choices of materials, construction techniques and design alternatives, the cheaper the better, while keeping the quality and efficiency a priority.

On top of those general design focus points, several specific design focus points are considered for each part of the condensing unit. They are presented in the following sections, together with the design alternatives and the choices made.

4.4.2 Extraction System

4.4.2.1 Plants Tank

The **primary function** of the plants tank is to contain a plants bed of 1 kg while allowing steam generated upstream to pass through it in an homogeneous way. The steam should be able afterwards to exit the cover towards the condensing unit. The steam condensing in the plants bed should be limited thanks to the use of a proper insulation of the walls. The tank should be cylindrical and its cover should be easily removable. The whole system should be entirely watertight against steam, but also to prevent the infiltration of red sand and dust coming from the outside.
The materials of the plants tank were determined in section 3.1. Some guidelines about sizing were drawn in section 3.2.7. Now practical solutions need to be analysed. The following **alternatives** were considered:

1. Initiate the manufacturing of a custom-made tank that fulfils all the requirements
2. Try to find a tank on the local market that corresponds the most to the requirements and adapt it afterwards

The first alternative is not feasible at the Atelier Central de Maintenance of the UO. Indeed, the available tools do not allow manufacturing a regular cylindrical tank with a watertight removable cover, in either of the selected materials. The possibility to hire a private contractor was considered. Seen the lack of information regarding the available manufacturing companies on site (no web sites are available), the limited timing reserved for the construction of the whole unit (six weeks) and the possibly high costs that it would generate, it was chosen not to pursue this alternative.

Figure 4.8: Hardware store where the pressure cooker was bought

It was thus chosen to buy an existing tank on the local market. As phenolics are not available on site (or at least the information is not available), the focus was on stainless steel tanks. Several small hardware stores were visited in the city to review the possibilities. It was found that the best candidates are stainless steel pressure cookers. Indeed, those are watertight and exist in various sizes. Their cover is easily removable. They should easily be adapted in the ACM workshops.
A stainless pressure cooker was bought at a local hardware store (see figure 4.8). It was selected on the basis of its small diameter (see table 4.4) and also after verifying the water tightness of the cover annular seal, the ease to remove and close the cover and its general state (no bumps, no wear, etc.).
The pressure cooker required some **adapting** in order to be inserted in the extraction circuit. On its bottom, a hole was pierced and a threaded galvanized steel connector (see figure 4.10) was

brazed in order to connect the plants tank with the water container. The cover was adapted too: a hole was pierced and a connector brazed to it. The latest connector was chosen in order to fit the tip of the condensing hoses of the existing unit. Unfortunately the only material available for this type of connectors on site is copper, although stainless steel was highly recommended as a consequence to the materials selection (section 3.1). However, the reality on site implies that part of the objectives cannot be achieved, and must be replaced by accessible solutions. Regarding the **insulating materials**, the two materials available on site are hard polystyrene foam and glass wool. As the insulation of the cylindrical part of the tank requires a flexible insulating material, glass wool was purchased and fixed around the plants tank with metallic wires (see figure 4.9). As glass wool was harder to fix on the tank cover, its profile was shaped in a recycled piece of hard polystyrene foam. The latter also allows insulating the first centimetres of the pipe linking plants tank to the condensing unit, in its vertical part.

Table 4.4 presents the dimensions of the plants tank subsystem of the new extraction unit.

Tank	$d_{\mathrm{t,site}} = 0.19$ [m]
	$e_{\mathrm{t,site}} = 0.004$ [m] (estimated)
Insulation	$e_{\mathrm{i}} = 0.02$ [m] (estimated, mean)

Table 4.4: Dimensions of the plants tank subsystem of the new extraction unit

Figure 4.9: Insulated pressure cooker

Finally, an important advantage of the tank selected is that it was sold with a stainless steel support drilled with small holes (see figure 4.11), having dimensions such that it can be inserted in the tank while being adjoining the tank walls. This corresponding perfectly to the requirements for the plants bed support, allowing for the penetration of steam inside the plants bed through multiple entrances. A small stainless steel hanging tool was also in the «package», recycled into an elevating system for the plants bed support (see figure 4.12). This, combined with the numerous holes of the plants bed support, should allow a good **homogenisation** of steam through the plants bed.

Figure 4.10: Bottom Connector

Figure 4.11: Plants bed support

Figure 4.12: Elevating system

4.4.2.2 Condensing unit

The **primary function** of the condensing unit is to condense and cool down the distillation products. The pipes processing the flow of distillation products should be watertight at the connections.

First, a simulation was run on the basis of the purchased tank diameter in order to determine the lowest radius of the condensing unit pipes such that the vapour flow of the distillation product inside the pipes has a Reynold number superior to 2100 (at least a transition flow is needed to limit the pipes total length, see section 3.2.6.2). It was found that any hose with an inner radius of less than 9 mm would be suitable - this includes the hoses of the existing extraction unit, whose radius is 6 mm (see table 4.2).
Therefore, given the good state of the existing **stainless steel hoses** (no corrosion, no wear) despite of their previous usage for the same application, and because their material is consistent with the materials selection performed in section 3.1, it was chosen to recycle the hoses of the existing extraction unit and use them for the new extraction unit. Indeed, this reduces the cost and it should be easy to buy additional hoses when necessary. At this point, it is worth noting that there is an important difference between the computed length of pipes necessary for the condensing and cooling of the distillate (about 15 m) and the length of hoses available on site, as used for the previous unit. Two main reasons can be identified:

- If the parabola of the previous extraction unit has a low efficiency, it is possible that the distillate mass flow rate present when running the previous extraction unit is lower than the mass flow rate resulting from an optimal sizing of the extractor. The available hoses length would then be sufficient for use in the previous extraction unit.
- Natural convection is hard estimate. However, this heat exchange mode plays an important role in the condensing process, as the hoses are placed in a tank full of stagnant water. Therefore, it is possible that an accuracy at the level of the natural convection heat transfer induced oversized computation results with respect to the pipes length.

Therefore, it was chosen not to purchase additional hoses until the unit was tested. The hoses length can easily be adapted afterwards, if it is shown that additional hoses are needed.

The copper **tap** allowing the products to exit the condensing unit was replaced by a stainless steel tap (see figure 4.13). Indeed, the materials selection in section 3.1 recommended to avoid copper for any pipe work, as it interacts with the distillation products. This was confirmed by the corroded state of the copper tap.
Regarding the **gaskets** ensuring the tightness of the condensing circuit at the connections between hoses, the old reddish gaskets were identified as a potential cause for the abnormal colouration of the essential oil extracted during the studies of 2012 [6] (see section 3.1.1).

Therefore, two alternatives were envisaged:

1. Try to find gaskets on site that would be consistent with the materials selection (section 3.1.3.7) or at least compatible with the distillation products (no interaction between seals and essential oils, temperature compatibility, etc.).

2. Buy gaskets in Belgium before leaving to Ouagadougou, that would fit the requirements. Those concern first the gasket material, but also their size that should be adapted to the hoses.

It was expected that the choice of gaskets materials on site would be very narrow. Therefore, it was chosen to buy several gaskets at a large hardware store[1] in Belgium prior to departure. The choice in materials was rather narrow: the two available gaskets materials were natural rubber and aramid fiber. As natural rubber was excluded upon the seals materials selection (see section 3.1.3.7), **aramid fiber gaskets** were chosen.
Indeed, the label of the gaskets indicating suitability for «cold and hot water-steam until 300°C, heater oil, acid, base, domestic gas (natural or liquefied)», they are expected to be suited for the present application, and more specifically to be durable with respect to essential oils. The choice of the gaskets size was made based on the available information about the dimensions of the existing hoses [6], and four packs of four 12 x 17 mm aramid fiber flat gaskets were purchased.
Moreover, two rolls of **polytetrafluoroethylene tape** (PTFE, trade name: Teflon) were bought in order to apply on the threaded parts of the hoses connectors and improve the tightness of the condensing circuit (see figure 4.14).

Figure 4.13: Taps: new stainless steel (left) and previous copper (right) - Aramid fiber gasket (upper right corner)

Figure 4.14: Teflon tape

Finally, the alternatives regarding the **condensing tank** were:

1. Purchase or order the construction of an aluminium tank that would resist corrosion by water and the outside environment indefinitely
2. Recycle the condensing tank of the existing unit

In order to limit the costs and because of the limited time frame, the second alternative is chosen. The inner walls of the **carbon steel condensing tank** were sandpapered in order to remove the rust, and a new coating of anti-rust paint is applied. This should be done at least once a year to ensure the durability of the condensing tank.

At the end of the construction phase, the entire condensing unit is mounted, and the tightness of each hoses connection is thoroughly tested, and the PTFE seals remade if necessary.

4.4.2.3 Separator

The separator of the existing extraction unit was designed and successfully used during the studies of 2012 [6]. Therefore, in the framework of this thesis, it was chosen to recycle it for the new extraction unit.

[1] Brico, <www.brico.be>

4.4.3 Vapour Generation System

4.4.3.1 Solar Concentrator

The **primary function** of the solar concentrator is to redirect the beam component of the solar radiation towards the solar collector, as efficiently as possible. Besides the optical properties, there are several important criteria to consider upon choosing the type of solar reflector:

- **Durability** with respect to outdoor exposure
- **Maintenance**
- **Cleaning**
- **Cost**
- **Availability**
- **Construction ease**
- **Construction duration**

The following alternatives were considered, once on site:

1. Glass mirrors, whose type would depend on the availability on site.
2. Aluminium sheet, whose manufacturing process would depend on the local manufacturers.

In order to make a final choice, each alternative is analysed with regards to the selection criteria. For each criterion, an index O is assigned, taking values on a scale from 1 to 5, according to an increasing degree of optimality with respect to the criterion considered. A second index P describing the degree of priority of the criterion is also assigned to each criterion, also on a scale from 1 to 5 according to an increasing degree of priority. A global index can finally be assigned to each candidate by computing the sum on all criteria of the products of O by P for each criterion.
The availability criterion is priorly analysed, in order to compare available candidates. On the one hand, the same mirrors as those used for the already existing unit are still available; their precise optical properties are however unknown. On the other hand, a sample aluminium sheet made by a local manufacturer is available at the ACM at the beginning of the stay. The same type of aluminium sheet was already used on site as a reflective surface for a parabolic dish solar cooker, successfully according to Adama Ouédraogo. The exact type of aluminium sheet and therefore its precise optical properties are however unknown.
Those two candidates are analysed in the following tables, on the basis of the results of the critical observation of the existing unit (section 4.2.2.1), literature data and personal reflections.

Glass mirrors			
Criterion	**Comment**	O	P
Optical properties	Unknown precisely. However, assuming silver glass mirrors, the overall optical properties are expected to be slightly better than those of an aluminium sheet (see section 3.2.4.2).	5	5
Durability	A study studying the influence of outdoor exposure through accelerated ageing of solar reflector materials showed that silver glass mirrors are amongst the candidates encountering the least degradation upon outdoor exposure [7]. However, if a chock causes glass fragments to wear off, then the mirrors specularity decreases drastically at the corresponding spot.	4	4
Maintenance	The high brittleness of glass generates important needs for punctual maintenance, to replace the broken mirrors if they are considerably damaged.	3	3
Cleaning	Water is sufficient.	5	2
Cost	Increases as a function of maintenance requirements.	3[2]	4
Construction ease	The need to find a new glue that sustains high temperature but does not corrode the mirrors reflector induces a major difficulty. Moreover, it is not certain that this type of glue exists on site.	1	3
Construction duration	The construction involves the cutting of the mirrors into pieces, the finding of a suitable glue, and the assembling phase.	1	4[3]
Global index		**79**	

Table 4.5: Assessment of the glass mirrors candidate

[2] The initial cost of the mirrors is not available. Therefore, the cost influence is not considered in the global choice, by imposing the same O index to the two candidates.

[3] The high priority index assigned to the construction duration is mostly due to the limited time frame of the author's stay on site. In other circumstances, it is conceivable to give less priority to the construction duration.

Aluminium sheet			
Criterion	**Comment**	*O*	*P*
Optical properties	Unknown precisely. However, the optical properties of aluminium reflectors were discussed in section 3.2.4.2, and are globally good.	4	5
Durability	Assuming that the reflector is an anodised aluminium sheet, a study studying the influence of outdoor exposure through accelerated ageing of solar reflector materials showed that this type of reflectors is amongst the candidates encountering the least degradation upon outdoor exposure [7].	5	4
Maintenance	No maintenance necessary until the lifetime of the aluminium sheet is passed.	5	3
Cleaning	A cleaning agent is required that does not corrode the aluminium sheet	4	2
Cost	The initial cost is rather high but does not increase with time.	3	4
Construction ease	The construction requires a suitable glue and a way to press the aluminium sheet to the parabolic profile during the whole duration of the glue drying process. Otherwise, concentrating losses occur.	3	3
Construction duration	It only involves the glue drying process.	5	4
Global index			**104**

Table 4.6: Assessment of the aluminium sheet candidate

The computation of the global indices (glass mirrors: 79, aluminium sheet: 104) allows choosing the **aluminium sheet** for the **reflective surface of the solar concentrator**.

Before sizing the parabola on the basis of the diameter of the plants tank, it is required to determine the **climatic working point** that would correspond to the dry season during the time of one extraction. On the basis of measurements made during the first days of the author's stay in Ouagadougou, the climatic working point is based on the following data: $T_{\text{atm}} = 40°C$, $F = 1000$ W/m^2 and $RH = 0.25$. Those data correspond to data that are expected to be available during the dry season, from 10.30 am to 1.30 pm (the hottest hours), this interval corresponding to the expected duration of one extraction. The on site determination was required because the only climatic data available concern monthly average values [14], and not the evolution of the parameters through the day. However, as only one extraction per day needs to be performed, the focus can be on the hottest hours and the clear sky days.

On the basis of the climatic working point, the diameter of the plants tank newly purchased and the other data corresponding to the working point of section 3.2.5, a prior simulation was run in order to determine the parabola surface required to produce the nominal superficial speed of steam through the plants bed. This allowed determining that **a parabolic surface of 1.5 m^2 is required**. Given this computation result, it was chosen to use to sample aluminium sheet of 1 x 1 m available at the ACM and order an additional piece of aluminium of the same width to put next to it. Given the curvature given to the aluminium sheet to stick to the parabolic profile, and arbitrary fixing the focus of the parabola at 50 cm, the width of the parabola could be computed such that the arc length[4] is 1 m, and is equal to 0.96 m. This allowed simulating the parabola sizing again using an iterative procedure that allowed

[4]The computation of the arc length of the parabola is presented in appendix C.

determining its final length. At the end, it was found that an additional piece of aluminium sheet of 58 cm should be ordered. However, only a piece of 46 cm could be obtained two weeks after the ordering, the company being apparently out of stock. This inducing a parabola surface reduction of less than 8 %, it should not cause any malfunctioning of the extraction unit.

On the basis of the focal distance and of the arc length computations, the parabolic profile is drawn and shaped on four wood planks of good quality, of a thickness of about 5 cm (see figure 4.15a). Those allow regular intervals along the parabola length, and are assembled with longitudinal supporting wood planks of the same type. A sheet of plywood of 5 mm is nailed down to the four parabolic in such a way that the parabolic profile is followed at any point of the plywood sheet.

The fixation of the two pieces of aluminium sheet is first attempted using numerous nail fixations all along the sheets (see figure 4.15b). However, it was observed that a lot of bumps were forming at the places where the sheets were not constrained. On the other hand, the nails induced local deviations of the reflected solar flux. It is therefore decided to glue the aluminium sheets to the parabolic profile. A Ms Polymer glue (label: Sader) is recommended by Justin, the carpenter. A quick research indeed shows that this kind of glue is ideal for the present application, because of its excellent durability and resistance to climatic hazards and high temperatures, while being adapted to all types of materials[5].
The optimal way to glue the aluminium sheets to the parabolic profile would be to use a press of the same parabolic shape as the parabolic profile, and keep the press applied until the glue is completely dry. However, the raw materials necessary to build this kind of press are not available at the ACM. In order to limit the costs, it is decided to cover the glued aluminium sheet with a cover, and then distribute heavy rocks across the parabola surface, that act like a press (see figure 4.16). After the gluing of the aluminium sheets, the bumps that were observed when they were simply nailed are less present. However, some important profile flaws remain (bumps, irregularities), due to the kind of press that was used when the glue was drying. Therefore, it is expected that the concentrating efficiency is lower than the one expected. This is confirmed later when the parabola is fixed to the global structure, and that the observation is made that a non negligible part of the reflected solar flux is not redirected towards the solar collector. Some testing at the end of the stay was performed in order to assess the parabola global efficiency (see section 4.5).

(a) Justin sawing the parabolic profile

(b) Nailed Al sheets - Removal of the protective film

Figure 4.15: Parabola construction progress

[5]This is claimed by the Fixall glue label, producing Ms Polymer glues: `http://www.fixall.eu/fixall/index.php?option=com_content&task=view&id=14&Itemid=98`

Figure 4.16: Improvised press for the glue drying duration

4.4.3.2 Solar Collector

The **primary function** of the solar collector is to absorb the solar radiation redirected towards it by the solar concentrator, in order to boil off the water contained inside it. In order to limit the heat losses, the positive impact of the construction of a glass greenhouse around the water container was shown in section 3.2.6.1.
The alternatives regarding the water container were:

1. order the manufacturing of an aluminium half-cylindrical container at a private contractor's

2. choose a material that could be shaped at the ACM with the available tools.

Figure 4.17: Water Container

Because of the lack of information about whether the first alternative was feasible and the costs that would follow, the second alternative was chosen, and the construction of a half-cylindrical tank was initiated from a low carbon steel sheet of 1.5 mm thickness. The first requirements about size were about 1.5 m length to match the parabola length, and a radius of about 5 cm, corresponding to twice the volume of water required for one extraction. During the construction, the workers found out that they could not bend the steel sheet as to obtain such a short diameter, without an appropriate bending machine that was not available at the workshop. Therefore, the final dimensions of the water container are larger than wanted, with a radius varying between 7 to 10 cm depending on the place of measurement (there are irregularities to the half-cylindrical profile). Following the model of the existing extraction unit, the top of the half-cylinder is inclined symmetrically with respect to the exit hole, to allow for the natural circulation of steam towards it, and make the action of emptying the water collector very easy. All the joining between sheet pieces is made using gas welding (see figure 4.17). A 4 mm thick reinforcing plate is welded at the center of the flat top, to allow piercing the exit hole without damaging the structure. A galvanized steel connector is welded into the hole, matching the plants tank connector.

The inside of the water container is wetted with anti-rust paint in order to enhance the water container durability (see figure 4.18a). The outside is coated with anti-rust and several layers of black mat paint, to enhance the absorptivity of the water container (see figure 4.18b).

As one of the noted failings of the solar collector was the fact that dirt was accumulating inside the greenhouse, decreasing the greenhouse wall transmittance and therefore increasing the heat losses. This dirt could not be washed unless the top glass plates of the greenhouse are disjointed by removing the silicon, which corresponds to damaging the structure each time cleaning is needed, and rebuild it afterwards. Therefore, it was chosen for the new extraction unit to envisage a removable greenhouse top. A wooden frame was imagined, constituted of two mating parts (one on the half-cylindrical part of the greenhouse, the other supporting the top glass plates). Hinges would link the mating parts on one side, and latches would allow to close the frame on the other side. A flat silicon seal would be applied on the lower part and dried, constituting a slightly compressible joint ensuring the possible spacing between the two mating parts to be sealed when the greenhouse is closed. Although a wooden frame would have allowed limiting the heat losses, a metallic frame is built, because of ease of manufacturing concerns expressed by the workers of the ACM (see figure 4.19a).

Steel half-cylindrical profiles are shaped and placed at the extremities and the center of the water collector (see figure 4.18a) in order to support the glass laths of the greenhouse. After computing the required glass surface from the profiles perimeter, 5 mm thick glass plates are ordered and cut into pieces of about 5 cm width and 70 cm length. Two wider plates are foreseen for the top. The laths are arranged along the half-cylindrical profile and the spacing between them is plugged with silicon.

In order to fix the solar collector to the global structure of the extraction unit, two 4 mm thick reinforcing plates are welded at the extremities, and a connecting piece is welded on them (see figure 4.17).

(a) Anti-rust coating

(b) Application of the black mat coating

Figure 4.18: Water Collector

Table 4.7 contains the different dimensions of the new solar collector. The radius of the metallic half-cylinder is an estimation of the radius mean value.

(a) Metallic frame and latches

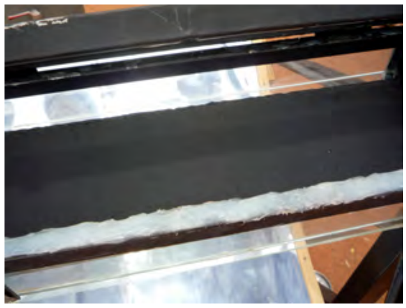

(b) Flat silicone seal

Figure 4.19: Greenhouse frame

Water container	$r_1 = 0.09$ [m] (estimated)
	$e_{\mathrm{m}} = 0.0015$ [m]
Air	$e_{\mathrm{a}} = 0.02$ [m] (estimated)
Greenhouse	$e_{\mathrm{g}} = 0.005$ [m]
Length	$L = 1.5$ [m]

Table 4.7: Dimensions of the solar collector of the new unit

4.4.4 Structure

In order to assemble and support all parts of the extraction unit, and also to allow for the continuous reorientation of the solar reflector as a function of the position of the sun, a supporting structure needs to be built, fulfilling the following requirements:

- easy to handle: light, easy to mount and dismount
- fully steerable: this involves the possibility to track the sun rotation and the sun «vertical» displacement
- robust

The items presented in this section result principally from construction choices recommended by Adama Ouedraogo, the head of the ACM. Indeed, the construction of the previous extraction unit gave him knowledge about the best solutions regarding ease of handling, parabola orientation and robustness.

Supporting vertical pillars are constructed from robust metallic rectangular tubes, as well as the bottom supporting structure (see figure 4.20). A support for the condensing tank is also built from metallic rectangular tubes of lower section. Round tubes are used to hang the parabola to the axis of the solar captor, with a loose connection allowing for the free rotation of the solar concentrator around it. This hanging structure is designed such that the focus of the parabola is at the bottom of the water container. The collector axis is attached to the vertical pillars through its threaded connectors (shown before on figure 4.17 of section 4.4.3.2). The connections allow fixing the position of solar collector when the unit is being used, while releasing them allows for the free rotation of the solar collector around its axis, which is necessary to empty it after each extraction.

In order to fix the position of the parabola with respect to the rotation around its focal axis, two counterweights are foundered in cement, and their position along two round tubes perpendicular to the parabola surface can be adapted thanks to moveable wedges.

Finally, five robust casters are mounted on the bottom supporting structure, to allow for the continuous tracking of the position of the sun during the whole extraction.

Figure 4.20: Structure of the extraction unit

4.4.5 Costs

Table 4.8 presents an overview of global cost of construction materials linked to each subsystem of the extraction unit.

Subsystem/part	**Cost** [CFA francs[6]]
Plants tank	**65500**
Main elements:	
Pressure cooker	25000
Insulation	13500
Solar collector	**146850**
Main elements:	
2 m^2 glass	30000
Low carbon steel sheet	25000
Solar reflector	**132500**
Main elements:	
1.5 m^2 aluminium sheet	60000
Wood planks and plywood	54000
Condensing unit	**16000**
Mostly recycled from the previous extraction unit	
Structure	**126850**
Total	**487700 CFA francs = 750 €**

Table 4.8: Costs

[6]The conversion rate is 1€= 650 CFA francs

It is worth noting that in the frame of this work, the manpower was free, in the framework of inter-university cooperation. This would not be the same in case of an independent reproduction of the prototype. An additional cost of about 250€ should then be foreseen, on the basis of three workers working full time during one month, with monthly salary of 60000 CFA francs.

4.5 Testing

Once the construction is concluded, five days remain to perform some testing on the prototype. The goal of this section is to confirm the model of the extraction unit developed in section 3.2. First, the greenhouse glass absorptivity is assessed. Second, the final dimensions and materials of all parts of extraction unit are updated and used to simulate the behaviour of the solar collector subsystem during the heating phase. Tests data allow then to determine the actual overall efficiency of the parabola, all other parameters being fixed.

4.5.1 Measurement Tools

The temperature measurements are performed using a Testo 905-T1 thermocouple, which accuracy is 1°C.

The solar flux measurements are performed using a Kimo SL100 solarimeter, which accuracy is 5% of measurement. The measurements of the direct solar flux are taken by changing the orientation of the measurement probe with respect to the sun, until the maximum value is found.

4.5.2 Greenhouse Glass Absorptivity

Once the construction is concluded, it is observed that even after careful cleaning, some stains remain on the greenhouse glass. It is therefore probable that the glass absorptivity is lower than the one used upon sizing computations ($a_{\mathrm{g}} = 0.05$, see section 3.2.5). The method used to measure the glass absorptivity is the following:

- Place the solarimeter probe against the greenhouse glass, inside the greenhouse, turned towards the outside. Take a steady-state flux measurement (F_{in}).
- As fast as possible, put the solarimeter probe at the same spot outside the greenhouse, while being careful that it has the same orientation as when it was inside the greenhouse. Take a steady-state flux measurement (F_{out}).
- Repeat the procedure at several spots of the greenhouse.

The comparison between the two flux measurements and averaging the results allows computing the glass absorptivity, given by $1 - \frac{F_{\mathrm{in}}}{F_{\mathrm{out}}}$. Table 4.9 presents the results of the five measurements that were performed. It also gives the resulting value of the glass absorptivity, which is used for the computations made in the following sections.

F_{in}	F_{out}	$\frac{F_{\text{in}}}{F_{\text{out}}}$
440	545	0.81
418	506	0.82
321	398	0.81
290	365	0.79
456	566	0.81
Glass absorptivity		0.19

Table 4.9: Measurement of the greenhouse glass absorptivity

4.5.3 Determination of the Overall Efficiency of the Parabola

4.5.3.1 Operating Method

In order to assess the actual value of the parabola overall efficiency, the vapour generation system is taken separately, and its behaviour studied during the heating phase of a certain mass of water contained in the tank. The operating method is the following:

- Pour 5 L of water inside the water container. Cover the vapour exit opening.
- Clean thoroughly the external walls of the glass greenhouse[7].
- Clean thoroughly the aluminium sheet surface.
- Measure the water temperature (beginning of the measurements).
- Every two minutes, measure the direct solar flux and the ambient temperature.
- Every ten minutes, measure the temperature of water in the solar collector.

4.5.3.2 Inaccuracy of Measurement

Despite the inaccuracy characteristic to the measurement tools, additional inaccuracy is introduced through the process of measuring the water temperature in the water container. Indeed, the thermocouple takes about 30 seconds to display a steady state value. As during the measurement, which total duration is about 30 seconds to one minute, the water collector opening needs to be opened, heat losses occur.
Moreover, the inaccuracy on the volume of water put in the tank is high, reaching 500 mL (water is introduced in the tank using a measuring container of 1 L five times which accuracy is 50 mL, and considering that sometimes water is lost when pouring it into the water container through the small opening, it was assessed that the accuracy on the water volume is 100 mL each time water is poured in the solar collector.

4.5.3.3 Heating Phase Analysis

The comparison between experimental results and model allows recovering the actual value of the parabola overall efficiency, all other parameters being fixed according to the dimensions and materials of each part and the measurement of the glass absorptivity. The simulations are run using the experimental data of direct solar flux and ambient temperature, adapted at each time loop of two minutes duration.
Only one test result is presented here, because it was the only of the two tests performed that was exploitable. Indeed, at the time of the second test, the sky was very cloudy, causing

[7]The internal walls cleaning needs to be done regularly (e.g. once a week), but not each time.

the direct solar flux to vary continuously over a wide range (from 500 to 1000). Therefore, considering a constant solar flux during each two minutes interval was far from reality, and sometimes steady-state flux measurements could not even be taken. However, the good fitting obtained on each portion of the experimental curve using close values of the overall efficiency allows confirming the admissibility of the test (see below).

Figure 4.21 shows the experimental measurements of the water temperature as a function of time. Simulation results are also plotted, using two values of the parabola efficiency that fit the experimental results the best. At the beginning of the heating phase, the best fitting is obtained with a parabola overall efficiency of 31%, while 30% fits the best at the end of the heating phase. A mean value of **30.5%** can thus be considered for the **actual overall efficiency of the parabola**. This value is much inferior to the 72% considered upon sizing the extraction unit (see section 3.2.4.2.2). This is a consequence of the important concentrating losses that are observed, and possibly the poor quality of the reflective aluminium sheet.

It is worth noting that right to the dashed red line on figure 4.21, the boiling temperature is reached. Therefore, the water temperature has reached a plateau, and the simulation fittings considering a heating phase are not applicable.
Figures 4.22a and 4.22b respectively show the evolution of the direct solar flux and the ambient temperature during the test.

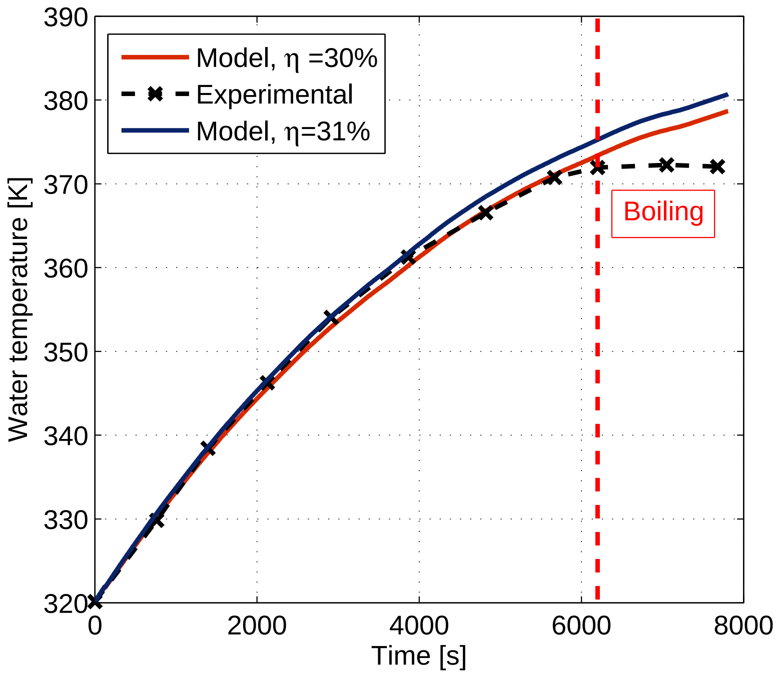

Figure 4.21: Fitting of the experimental data during the heating phase by adjusting the parabola efficiency

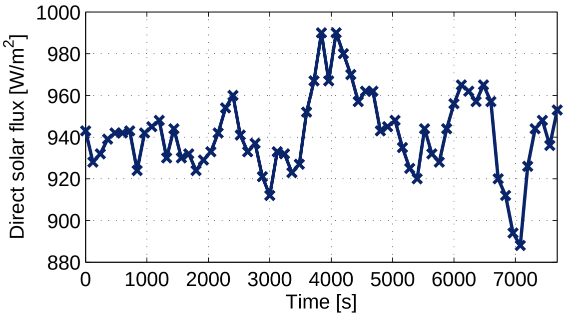

(a) Direct solar flux measurements

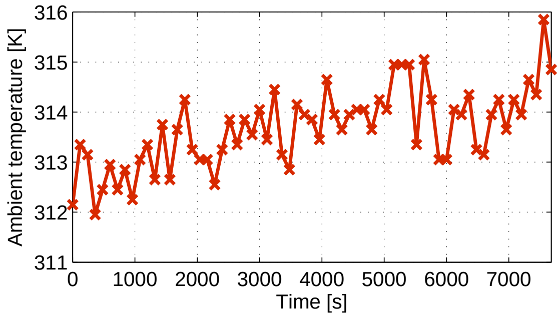

(b) Ambient temperature measurements

Figure 4.22: Parabola efficiency - Experimental data for the solar flux and the ambient temperature

Running a simulation with the adapted value of the parabola efficiency and assuming a climatic working point corresponding to $T_{\text{atm}} = 40°\text{C}$, $F = 1000$ W/m^2 and $RH = 0.25\%$ shows that the resulting steam superficial steam through the plants bed is far too low, and is equal to $3.4 * 10^{-3}$ m/s. This is much lower than the lower boundary of the steam superficial speed, which is $14.2 * 10^{-3}$ m/s (as presented in section 3.2.5). This result, caused by the poor quality of the parabola constructed, indicates that the unit should be improved before an optimal use is possible.

4.5.3.4 Case of the Glass Mirrors of the Previous Unit

For the sake of completeness, and seen the poor overall efficiency obtained with the aluminium sheet, the same heating test is performed on the previous extraction unit. The fitting of the experimental data with simulation results allows determining that the overall efficiency of the glass mirrors parabola is even worse than the efficiency of the aluminium sheet, and corresponds to 28%. This confirms the poor state of the reflective surface observed on site (as presented in section 4.2).

4.5.4 Quality of Distillation Products

The extraction unit was first run several times with water and no plants, in order to first assess the quality of the condensed water. It resulted in a perfectly clear water. This is a positive outcome, indicating compatibility between steam and the extraction unit materials.

An oils extraction was then attempted from *Eucalyptus* leaves. The poor climatic condition (low direct solar flux) and the low overall efficiency of the parabola caused that no oil could be extracted during the duration of the test, or at least in such negligible quantities that it could not be perceived. However, the distilled water contained dissolved plants extracts, as indicated by its odour. The collected water was still perfectly clear. This gives an indication about materials compatibility, assuming that the dissolved components have the same corrosion properties with respect to the unit materials than the oils themselves.

Chapter 5

Conclusions and Perspectives

5.1 Conclusions

The subject of this thesis is linked to the inter-university cooperation that exists between the Université libre de Bruxelles and the Université de Ouagadougou (UO). This work aimed at contributing to the research on essential oils that is performed on site for medicinal applications, by constructing an efficient extraction unit, whose materials are compatible with the essential oils compounds and the process parameters (e.g. temperature) and environment.

The project started with the preliminary study of an extraction unit using steam distillation and solar energy.
First, the materials for all parts of the extraction unit were selected using the Cambridge Engineering Selector Edupack Software. The selection was based on global criteria such as price and availability, and the analysis specific to each subsystem of its function, environment, requirements and constraints. Amongst the principal constraints, corrosion properties of materials were investigated, with respect to water and essential oils, and especially the corrosion properties of metals. At the end of the materials selection, a list of materials was provided for each subsystem of the extraction unit, with alternatives in case of lack of availability.
Second, a complete model of the heat exchanges occurring in every parts of the extraction unit was established, in order to serve as a sizing tool for the different subsystems of the unit. More particularly, a model of the steam generation system was established in order to predict what parabola surface is required to produce the necessary steam superficial speed through the plants bed, as a function of the plants tank diameter. A sensitivity analysis was finally performed in order to assess the influence of the main environment and process parameters, such as the direct solar flux, the overall efficiency of the parabola and the diameter of the condensing pipes. It also allowed drawing guidelines for the construction of a prototype.

Finally, the construction of an extraction unit prototype was managed at the Université de Ouagadougou, during a six weeks stay. Construction alternatives were considered for each part, and discussed with Adama Ouedraogo, the head of the Atelier Central de Maintenance (ACM) of the UO. A plants tank was bought first, and the sizing of the unit performed on the basis of its diameter. Each part was constructed in the respect of the materials selection and the sizing results, when it was possible. The construction was completed in about five weeks. The biggest challenge regarding the on-site construction was the very limited access to information. Indeed, specialized construction contractors and hardware stores do not have websites, and the only source of information was the knowledge of the workers of the ACM on the corresponding subject. Therefore, finding specific materials or pieces was difficult, as well as a manufacturer for parts that could not be manufactured with the tools of the ACM.

Therefore the options in construction choices were rather limited.
Once the construction was completed, some testing was performed on the extraction unit. First the vapour generation system was studied during its heating phase. The model allowed successfully fitting the experimental results of the water temperature evolution, once the parabola efficiency was adapted. The latter was shown to be lower than expected, due to the poor quality of the aluminium sheet used as a reflective surface, and the construction methods that were used. Running a simulation also showed that the resulting superficial speed of steam through the plants bed would be insufficient. Therefore, the unit could only be used in an optimal way if the parabola efficiency is improved first.
A heating test was performed on the previous extraction unit in order to compare the parabola overall efficiencies of the two units. The resulting determination of the overall efficiency of the glass mirrors reflector appeared to be even lower than the efficiency of the aluminium sheet reflector. Therefore, no better results would have probably been obtained if glass mirrors of the same quality had been chosen instead of aluminium sheets.

5.2 Perspectives

5.2.1 Technical Aspects of the Constructed Extraction Unit

The first important technical perspective regards the solar reflector. Indeed, it the framework of this thesis, it was chosen to use an aluminium sheet reflector locally manufactured. This choice was based on a set of advantages that this kind of reflector offered compared to glass mirrors, principally in the fields of durability, maintenance and ease of construction. Moreover, the parabola of the previous extraction unit being made out of glass mirrors, it was interesting to test the other identified alternative that constituted the aluminium sheet. Finally, a large piece of aluminium sheet of 1 m^2 was already available at the ACM at the beginning of the stay.
As the testing of the vapour generation system showed that the performances of the parabola constructed are insufficient, it is needed to first improve the reflective and/or concentrating potential of the parabola before an optimal use of the extraction unit is possible. Several options can be considered:

- Re-glue the aluminium sheet on the parabolic profile using an appropriate press, in order for the reflective sheet to perfectly fit the profile. This would allow decreasing the concentrating losses, visually observed on site after construction.

- If the first solution is not sufficient, a new parabola of adapted surface could be designed using the same aluminium sheet reflector type. The model developed in the framework of this thesis would allow computing the adequate surface, taking into account the overall efficiency of the parabola recovered from the testing of the vapour generation system.

- Finally, the third solution would be to use a different type of reflective material. As the glass mirrors used on the previous unit appeared to contribute to a bad parabola overall efficiency as well, it could be investigated if reflectors of better quality are available on site.

An other technical perspective regards the copper connector remaining in the extraction unit. In order to ensure full compatibility between essential oils and the materials of the unit, it should be replaced by a stainless steel connector. The latter could be purchased in an other country, as it appeared not to be available in Burkina Faso.

5.2.2 Use of the Constructed Extraction Unit

Once the performances of the parabola improved, the constructed extraction unit aims at being used for didactic and research purpose at the Université de Ouagadougou. Indeed, it should on the on hand be used as a laboratory prototype for students studying organic chemistry or solar technologies. On the other hand, it should allow producing essential oils for laboratory analysis and characterisation, and also characterising the oils extraction process of several plants species compatible with the steam distillation process.

5.2.3 Prototypes Construction

One of the main limits encountered upon the construction of the extraction unit prototype was the lack of access to useful information. Indeed, this caused to choose default solutions, without being certain that other envisaged construction alternatives regarding materials and construction techniques were not available. It would be interesting, if a new prototype of any kind should be constructed again in the same framework of development cooperation, to schedule a two weeks time frame dedicated to the investigation of all possible construction alternatives, with the help of Adama Ouedraogo, head of the ACM.

5.2.4 Development Cooperation

The Belgian Commission universitaire pour le Développement (CUD) recently announced that they were withdrawing in 2014 their inter-university cooperation program from Burkina Faso for the next three years period. However, a new thesis subject for 2014 in collaboration with the UO was proposed again by the cooperation development cell of the Université libre de Bruxelles, on the solar drying process in food applications. Moreover, the studies on essential oils in the framework of development cooperation will be pursued through a Master thesis dedicated to the characterisation of the extraction process of citronella essential oils, involving a stay in Cambodia to study the influence of several raw plants material characteristics.

Bibliography

[1] The Engineering Toolbox. URL `http://www.engineeringtoolbox.com/`.

[2] Michael F. Ashby. *Materials Selection in Mechanical Design.* Butterworth-Heinemann, Burlington, fourth edition, 2011.

[3] World Bank. Burkina Faso Data, 2013. URL `http://data.worldbank.org/country/burkina-faso#cp_wdi`.

[4] World Bank. Burkina Faso Country Brief, 2013. URL `http://web.worldbank.org/WBSITE/EXTERNAL/COUNTRIES/AFRICAEXT/BURKINAFASOEXTN/0,,menuPK:343886~pagePK:141132~piPK:141107~theSitePK:343876,00.html`.

[5] Bachir Benjilali. Chapitre 2 : Extraction des plantes aromatiques et médicinales - cas particulier de l'entraînement à la vapeur d'eau et ses équipements. In *Huiles Essentielles : De la Plante à la Commercialisation*. Corporation LASEVE. URL `http://corpolaseve.uqac.ca/manuel/`.

[6] Sacha Breyer. Etude du procédé d'extraction d'huiles essentielles par entraînement à la vapeur d'eau et optimisation d'une unité d'extraction solaire à l'Université de Ouagadougou. Master's thesis, Université libre de Bruxelles, 2012.

[7] Maria Brogren, Björn Karlsson, Anna Werner, and Arne Roos. Analysis of the effects of outdoor and accelarated ageing on the optical properties of reflector materials for solar energy applications. *Solar Energy Materials and Solar Cells*, 82(4):491–515, 2004.

[8] Jean-Marie Buchlin. *Phénomènes de Transports*. Université libre de Bruxelles, 2005. Course notes, Ecole Polytechnique de Bruxelles.

[9] Yunus A. Cengel. *Heat Transfer: A Practical Approach.* McGraw-Hill, New York, second edition, 2003.

[10] Thermal-Fluid Central. Natural convection on cylinders and spheres. URL `https://www.thermalfluidscentral.org/encyclopedia/index.php/Natural_convection_on_cylinders_and_spheres`.

[11] Avinash Chandra and R.P. Chhabra. Effect of prandtl number on natural convection heat transfer from a heated semi-circular cylinder. *International Journal of Chemical and Biological Engineering*, 6:69–75, 2012.

[12] CES Edupack. Cambridge Engineering Selector database, 2011.

[13] Aperam Stainless Europe. Stainless Steel and Corrosion. Technical report, Arcelor Mittal, 2010.

[14] FAOClim. Faoclim 2 world-wide agroclimatic database, version 2.01, 2011.

[15] D. G. Friend. Technical guidance document: Volatile treatments for the steam-water circuits of fossil and combined cycle/hrsg power plants. Technical report, The International Association for the Properties of Water and Steam, Canada, 2010.

[16] Jean Garnero. Huiles essentielles. *Techniques de l'Ingénieur*, 1996.

[17] Solar Energy Research Institute. Silver/glass mirrors for solar thermal systems. Technical report, Washington, 1985.

[18] John Kabuba and Robert Huberts. Steam extraction of essential oils: Investigation of process parameters. *The Canadian Journal of Chemical Engineering*, 87(6):915–920, 2009.

[19] Brian M. Lawrencet. Essential oils: From agriculture to chemistry. *International Journal of Aromatherapy*, 10(3):82–98, 2001.

[20] Lenntech. The chemical elements and water. URL `http://www.lenntech.com/periodic/water/overview.htm`.

[21] John H. Lienhard. *A Heat Transfer Textbook*. Phlogiston Press, Cambridge Massachusetts, third edition, 2008.

[22] E. Marston. Piping joint handbook. Technical report, Forties Field Group, 2000.

[23] Phineas Masango. Cleaner production of essential oils by steam distillation. *Journal of Cleaner Production*, 13:833–839, 2005.

[24] H.A. Mohammed and Y.K. Salman. Experimental investigation of mixed convection heat transfer for thermally developing flow in a horizontal circular cylinder. *Applied Thermal Engineering*, 27(8):1522–1533, 2007.

[25] Organisation mondiale de la Santé. Aperçu de la stratégie de coopération, 2009. URL `http://www.who.int/countries/bfa/fr/`.

[26] Lawrence E. Murr. *Solar Materials Science*. Technology & Engineering. Elsevier, 1980.

[27] Valspar Packaging. Steel Container Products, 2011.

[28] Marius Paulescu, Eugenia Paulescu, Paul Gravila, and Viorel Badescu. Chapter 2 : Solar radiation measurements. In *Weather Modeling and Forecasting of PV Systems Operation*, Green Energy and Technology. Springer-Verlag, London, 2013.

[29] Max Reboul. Corrosion des alliages d'aluminium. *Techniques de l'Ingénieur*, 2005.

[30] Marc Ringuette. Absorptivity and emissivity table. URL `http://www.solarmirror.com/fom/fom-serve/cache/43.html`.

[31] Carl Schoen. A new empirical model of the temperature-humidity index. *Journal of Applied Meteorology*, 4(9):1413–1420, 2005.

[32] Maxime Van Peel. Modélisation du procédé d'extraction d'huile essentielle par entraînement à la vapeur et développement d'un prototype d'extracteur solaire à l'Université de Ouagadougou. Master's thesis, Université libre de Bruxelles, 2011.

Appendix A

Air and Water Properties

Property	Unit	Value
C_p	$[\mathrm{J.(kg.K)^{-1}}]$	1009
ρ	$[\mathrm{kg.m^{-3}}]$	1.067
k	$[\mathrm{W.(m.kg)^{-1}}]$	0.0285
ν	$[\mathrm{m^2/s}]$	18.9e-6
β	$[\mathrm{K^{-1}}]$	3e-3

Table A.1: Air properties at 60°C

Property	Unit	Value
C_p	$[\mathrm{J.(kg.K)^{-1}}]$	1005
ρ	$[\mathrm{kg.m^{-3}}]$	1.127
k	$[\mathrm{W.(m.kg)^{-1}}]$	0.0271
ν	$[\mathrm{m^2/s}]$	16.97e-6
β	$[\mathrm{K^{-1}}]$	3.2e-3

Table A.2: Air properties at 40°C

Property	Unit	Value
L_vap	$[\mathrm{J/kg}]$	2257e3
C_p	$[\mathrm{J.(kg.K)^{-1}}]$	4179
ρ_vap	$[\mathrm{kg.m^{-3}}]$	0.59794
ρ_liq	$[\mathrm{kg.m^{-3}}]$	992.22
k_vap	$[\mathrm{W.(m.kg)^{-1}}]$	0.025
k_liq	$[\mathrm{W.(m.kg)^{-1}}]$	0.58
μ_vap	$[\mathrm{Pa.s}]$	12.268e-6
ν_liq	$[\mathrm{m^2/s}]$	0.553e-6
β	$[\mathrm{K^{-1}}]$	2.14e-4

Table A.3: Water properties at 1atm - liquid data at 40°C

Appendix B

Model Implementation: Matlab Codes

Main file : sizing

```
%% Thesis : Sizing of the Extractor

%% Thermodynamic Data

Water.L_vap=2257*1000; %[J/kg] Latent heat of vaporization at 1atm - ref:nist
Water.C_p=4179; %[J/K/kg] Heat capacity. constant pressure (1 atm, ...
    40degC) - ref:nist
Water.rho_vap=0.59794; %[kg/m^3] Density - ref:nist
Water.rho_liq=992.22; %[kg/m^3] Density at 40degC
Water.thermal_cond_vap=0.025; %[W/m/kg] 1atm - ref:nist
Water.thermal_cond_liq=0.58; %[W/m/kg] - engineering toolbox
Water.mu_vap=12.268e-6; %[Pa s]
Water.nu_vap=Water.mu_vap/Water.rho_vap;
Water.beta= 2.14e-4; %[/K] engineering toolbox
Water.nu_liq=0.553e-6; %[m^2/s] engineering toolbox at 50degC
Water.mu_liq=Water.nu_liq*Water.rho_liq;

%Air properties at 60degC
Air60.C_p=1009;
Air60.rho=1.067;
Air60.thermal_cond=0.0285;
Air60.nu=18.9e-6;
Air60.mu=Air60.nu*Air60.rho;
Air60.beta=3e-3;

Air.beta=3.2e-3; %[/K] engineering toolbox at 40degC
Air.rho=1.127; %[kg/m^3] engineering toolbox at 40degC
Air.C_p=1005; %[J/(K kg)] engineering toolbox at 40degC
Air.nu=16.97e-6; %[m^2/s] engineering toolbox at 40degC
Air.thermal_cond=0.0271; %[W/m/K] engineering toolbox at 40degC
Air.mu=Air.nu*Air.rho;

sigma_Boltzman=5.6703e-8;

%% Materials properties

Alu.cond=200; %[76-235][W/mK]
Alu.reflectivity=0.85; % Alu sheet
Alu.absorptivity=1-Alu.reflectivity; % Alu sheet
Alu.emissivity=0.09; %Alu sheet

Wood.cond=0.15; %[0.15-0.19][W/mK]
```

```
Glass.cond=0.7; %[0.7-1.3][W/mK]
Glass.absorptivity=0.05;
Glass.emissivity=0.9;

WoolGlass.cond=0.04;

StSteel.cond=17; %[W/mK] Stainless steel 340
Ststeel.rho=7700; %[kg/m^3] Stainless steel 340
Ststeel.C_p=490; %[J/kg/K]  Stainless steel 340

Black.emissivity=0.9;
%% Site data

% Climate
Site.p_atm=1; %[atm]
Site.T_atm=40; %[degC]
Site.RH=0.3; %[-]
Site.gamma_coeff=17.27*Site.T_atm/(237.3+Site.T_atm)+log(Site.RH);
Site.T_dp=237.3*Site.gamma_coeff/(17.27-Site.gamma_coeff);
Site.T_atm=Site.T_atm+273.15; %[K]
Site.time=12; %[h] hour after midnight
Site.T_sky=Site.T_atm*(0.711+0.0056*Site.T_dp+7.3e-5*Site.T_dp^2+...
    0.013*cos(2*pi*Site.time/24))^(1/4);
Site.solar_flux=1000; %[W/m^2]

% First thing to buy
Site.tank_diam=0.19; %[m]
%% Predeterminations

Lab.heating_power=0.5*500; %[W]
Lab.tank_diam=0.1; %[m]
Lab.tank_section=pi/4*Lab.tank_diam^2; %[m^2]
Lab.vapor_flowrate=Lab.heating_power/Water.L_vap; %[kg/s]

% Objectives and arbitrary data
Site.M_p=1; %[kg] plants mass
Site.t_ex=3*3600; %[s] Extraction time; counting from water evaporation


Site.tank_section=pi/4*Site.tank_diam^2; %[m^2]
Site.vapor_flowrate=Site.tank_section/Lab.tank_section*Lab.vapor_flowrate; ...
    % [kg/s]
Site.mass_water=Site.vapor_flowrate*Site.t_ex; %[kg] Mass of water to put ...
    in the tank
Site.steam_sup_speed=Site.vapor_flowrate/Site.tank_section/Water.rho_vap;

%% Plants data

%% Parabola

% Parabola Overall Efficiency

mirror=0;

if mirror==1;
    Parabola.efficiency=0.78;
else
    Parabola.efficiency=0.72;
end
```

```
Parabola.heat_flux=Parabola.efficiency*Site.solar_flux;

% Computation of the surface temperature of the parabola for a fully
% insulated Aluminium reflective surface

% Dimensions
Parabola.L=1.58;
Parabola.Al_thickness=0.001;
Parabola.ins_thickness=0.1;

% Conductivity coefficients
Parabola.hcond_Al=Alu.cond/Parabola.Al_thickness;
Parabola.hcond_ins=WoolGlass.cond/Parabola.ins_thickness;

%Temperatures initialisation
T_o=Site.T_atm; % temperature of the bottom surface of the insulation
T_i=50+273.15; % temperature at the interface between insulation and ...
    reflective surface
T_p=T_i+Parabola.hcond_ins/Parabola.hcond_Al*(T_i-T_o); %Temperature of ...
    the reflective surface
h_parabola=Parabola_losses(T_p,Site,Parabola,Air,mirror);
T_i=T_p-(Alu.absorptivity*Site.solar_flux...
    -(h_parabola.rad*(T_p-Site.T_sky)...
    +h_parabola.conv*(T_p-Site.T_atm)))/Parabola.hcond_Al;
ΔT=1;
while ΔT>0.01
    T_p_new=T_i+Parabola.hcond_ins/Parabola.hcond_Al*(T_i-T_o);
    ΔT1=abs(T_p_new-T_p);
    T_p=T_p_new;
    h_parabola=Parabola_losses(T_p,Site,Parabola,Air,mirror);
    T_i_new=T_p-(Alu.absorptivity*Site.solar_flux...
        -(h_parabola.rad*(T_p-Site.T_sky)...
        +h_parabola.conv*(T_p-Site.T_atm)))/Parabola.hcond_Al;
    ΔT2=abs(T_i_new-T_i);
    ΔT=max(ΔT1,ΔT2);
end
Parabola.T_i=T_i;
Parabola.T_p=T_p;
Losses=h_parabola.conv*(T_p-Site.T_atm)+h_parabola.rad*(T_p-Site.T_sky)...
    +Parabola.hcond_Al*(T_p-T_i);
Losses_down=Parabola.hcond_Al*(T_p-T_i);
Losses_up=h_parabola.conv*(T_p-Site.T_atm)+h_parabola.rad*(T_p-Site.T_sky);
Parabola.percent_cond=Losses_down/Losses*100;
Parabola.percent_heat_losses=Losses/Site.solar_flux*100;
clear T_o T_i
%% Captor
% In regime : losses + parabola efficiency
Material_captor=Alu;
% Dimensions
Captor.volume=Site.mass_water/Water.rho_liq;
Captor.L=Parabola.L;
Captor.r1=sqrt(2*Captor.volume/Captor.L/pi);
%Captor.r1=0.09;
r1=Captor.r1;
Captor.em=0.0015;
r2=r1+Captor.em;
Captor.eair=0.02;
r3=r2+Captor.eair;
Captor.eg=0.005;
r4=r3+Captor.eg;
```

```
Captor.D=2*r4;
S1=pi*r1*Captor.L+2*r1*Captor.L;
S2=pi*r2*Captor.L+2*r2*Captor.L;
S3=pi*r3*Captor.L+2*r3*Captor.L;
S4=pi*r4*Captor.L+2*r4*Captor.L;

% Regime
Captor.Te=273.15+100;
Captor.Tm=Captor.Te...
    +Water.L_vap*Site.vapor_flowrate/Material_captor.cond/Captor.L...
    /(pi/log(r2/r1)+2*r1/(r2-r1));

ag=Glass.absorptivity;
Fp=Parabola.heat_flux;
L=Captor.L;
km=Material_captor.cond;
Tm=Captor.Tm;
Te=Captor.Te;
kair=Air.thermal_cond;
sig=sigma_Boltzman;
epsm=Black.emissivity;
epsg=Glass.emissivity;
D=Captor.D;
Tatm=Site.T_atm;
betaair=Air.beta;
kg=Glass.cond;
rhoair=Air.rho;
Cpair=Air.C_p;
nuair=Air.nu; %[m^2/s] engineering toolbox at 40degC
muair=nuair*rhoair;

%Effective conductivity
L_c=Captor.eair;
Fcyl=(log(r3/r2))^4/L_c^3/((2*r2)^(-3/5)+(2*r3)^(-3/5))^5;
Prandtl_air60=Air60.mu*Air60.C_p/Air60.thermal_cond;
kair60=Air60.thermal_cond;
kaircoeff=kair60*0.386*(Prandtl_air60/(0.861+Prandtl_air60))^(1/4)...
    *Fcyl^(1/4)*(Prandtl_air60*9.81*Air60.beta*L_c^3/Air60.nu^2)^(1/4); ...
    % only to be multiply by (Captor.Tm-Greenhouse.Tv1)^(1/4)
Tsky=Site.T_sky;

% System solving - required surface of parabola
% Iterative solver
syms Sp Tv1 Tv2
sol=vpasolve([(1-ag)*(Fp*Sp)==km*(Tm-Te)*(pi*L/log(r2/r1)+2*L*r1/(r2-r1))...
    +kaircoeff*(Tm-Tv1)^(1/4)*(Tm-Tv1)*L*(pi/log(r3/r2)+2*r2/(r3-r2))...
    +sig*(Tm^4-Tv1^4)*S2/(1/epsm+S2/S3*(1-epsg)/epsg),...
    sig*(Tm^4-Tv1^4)*S2/(1/epsm+S2/S3*(1-epsg)/epsg)+ag*Fp*Sp...
    +kaircoeff*(Tm-Tv1)^(1/4)*(Tm-Tv1)*L*(pi/log(r3/r2)+2*r3/(r3-r2))...
    ==epsg*sig*(Tv2^4-Tsky^4)*S4+(Tv2-Tatm)*S4*0.78*(muair*Cpair/kair)...
    ^(0.27)*(9.81*betaair*D^3*(Tv2-Tatm)/nuair^2)^(0.2)*kair/D,...
    kg*(Tv1-Tv2)*L*(pi/log(r4/r3)+2*r3/(r4-r3))+ag*Fp*Sp...
    ==epsg*sig*(Tv2^4-Tsky^4)*S4+(Tv2-Tatm)*S4*0.78*(muair*Cpair/kair)^0.27...
    *(9.81*betaair*D^3*(Tv2-Tatm)/nuair^2)^(0.2)*kair/D],[Sp,Tv1,Tv2]);
kaireff=kaircoeff*(Tm-eval(sol.Tv1))^(1/4);
% Parabola Surface required
Parabola.Surface=eval(sol.Sp);
Greenhouse.Tv1=eval(sol.Tv1);
Greenhouse.Tv2=eval(sol.Tv2);

```

```
clear Sp Tv1 Tv2 Tm Te Tw

% Heating phase computation
Diam=D;
Mw=Site.mass_water;
Cpw=Water.C_p;
Sp=Parabola.Surface;
Δt=5; %[s]
Tw_vect(1)=Site.T_atm+4;
Tw=Tw_vect(1);
n=1;
timeheating(1)=0;

while Tw<100+273.15
    syms Tv1 Tv2 Twf Tm
    sol2=vpasolve([km*(Tm-Tw)*L*(pi/log(r2/r1)+2*r1/(r2-r1))*Δt...
        ==Mw*Cpw*(Twf-Tw),(1-ag)*(Fp*Sp)==km*(Tm-Tw)*(pi*L/log(r2/r1)...
        +2*L*r1/(r2-r1))+kaircoeff*(Tm-Tv1)^(1/4)*(Tm-Tv1)*L*(pi/log(r3/r2)...
        +2*r2/(r3-r2))+sig*(Tm^4-Tv1^4)*S2/(1/epsm+S2/S3*(1-epsg)/epsg),...
        sig*(Tm^4-Tv1^4)*S2/(1/epsm+S2/S3*(1-epsg)/epsg)+ag*Fp*Sp...
        +kaircoeff*(Tm-Tv1)^(1/4)*(Tm-Tv1)*L*(pi/log(r3/r2)+2*r3/(r3-r2))...
        ==epsg*sig*(Tv2^4-Tsky^4)*S4+(Tv2-Tatm)*S4*0.78*(muair*Cpair/kair)...
        ^(0.27)*(9.81*betaair*D^3*(Tv2-Tatm)/nuair^2)^(0.2)*kair/D,...
        kg*(Tv1-Tv2)*L*(pi/log(r4/r3)+2*r3/(r4-r3))+ag*Fp*Sp...
        ==epsg*sig*(Tv2^4-Tsky^4)*S4+(Tv2-Tatm)*S4*0.78*(muair*Cpair/kair)...
        ^(0.27)*(9.81*betaair*D^3*(Tv2-Tatm)/nuair^2)^(0.2)*kair/D],...
        [Tm,Tv1,Tv2,Twf]);
    Tm_vect(n)=eval(sol2.Tm);
    Tv1_vect(n)=eval(sol2.Tv1);
    Tv2_vect(n)=eval(sol2.Tv2);
    n=n+1;
    Tw_vect(n)=eval(sol2.Twf);
    Tw=Tw_vect(n)
    timeheating(n)=timeheating(n-1)+Δt;
    clear Tv1 Tv2 Twf Tm sol2
end


clear ag F L r1 km Tm Te r2 r3 r4 kair sig epsm S1 S3 epsg Tatm Cpair ...
    muair nuair rhoair betaair D kg

%% Tank
Material_tank=StSteel;
Material_insulation=WoolGlass;
% Dimensions
Tank.diam=Site.tank_diam; %[m]
Tank.height=1.5*Site.tank_diam; %[m]
Tank.wall_thickness=0.005; %[m]

Tank.superficial_fluid_velocity=Site.steam_sup_speed; %[m/s]

Insulation.thickness=0.05; %[m] ???

r1=Tank.diam/2;
r2=r1+Tank.wall_thickness;
r3=r2+Insulation.thickness;

Plants.C_p=1400; %[KJ/K/kg] value for cupboard - ref:CES
heat_plants=Site.M_p*Plants.C_p*(100+273.15-Site.T_atm);

```

```
% Losses - Stationary
solEnergy=0.9*800;

% As T_sky is different from T_atm, the vpasolve function is used again
% instead of the equivalent resistances method.

T_m=373.15;
syms Ti To CondensFR
eps=0.94;
h_rad=sigma_Boltzman*eps*(Site.T_sky^2+To^2)*(Site.T_sky+To);
Grashof_tank=9.81*Air.beta*Tank.height^3*(To-Site.T_atm)/Air.nu^2;
Prandtl_tank=Air.mu*Air.C_p/Air.thermal_cond;
Raleigh_tank=Grashof_tank*Prandtl_tank;
Nusselt_tank=4/3*(7/5*Raleigh_tank*Prandtl_tank/(20+21*Prandtl_tank))^(1/4)...
    +4/35*(272+315*Prandtl_tank)*Tank.height/(64+63*Prandtl_tank)...
    /(Tank.diam+2*Tank.wall_thickness+2*Insulation.thickness);
h_conv=Nusselt_tank*Air.thermal_cond/Tank.height;

sol3=vpasolve([CondensFR*Water.L_vap...
    ==Material_tank.cond/log(r2/r1)*(T_m-Ti)*2*pi*Tank.height,...
    Material_tank.cond/log(r2/r1)*(T_m-Ti)==...
    Material_insulation.cond/log(r3/r2)*(Ti-To),...
    Material_insulation.cond/log(r3/r2)*(Ti-To)*2*pi*Tank.height...
    ==(h_rad*(To-Site.T_sky)+h_conv*(To-Site.T_atm))*2*pi*r3*Tank.height],...
    [CondensFR,To,Ti]);

% Condensed flow rate
Tank.CondensFR=eval(sol3.CondensFR);
Tank.CondensPercent=Tank.CondensFR/Site.vapor_flowrate;
Tank.flowrate_out=Site.vapor_flowrate;

%% Condensing Unit

Material_condens=StSteel;

% Dimensions
Condens.radius=0.006;
Condens.thickness=0.001;
Condens.ΔL=0.01;

CondensTank.T=50+273.15;
Condens.toCondens=Tank.flowrate_out*Water.L_vap;
Condens.superficial_speed=Tank.flowrate_out/Water.rho_vap/...
    (pi*Condens.radius^2);

Condens.Reynolds=Condens.superficial_speed*2*Condens.radius/Water.nu_vap;
Grashof=9.81*Water.beta*(2*Condens.radius)^3*20/Water.nu_liq^2;
Richardson=Grashof/Condens.Reynolds^2;

Extract.T=100+273.15;
Condens.T_m=Extract.T-1;
Condens.T_ext=Extract.T-2;

% Indicating if the vapor is already condensed or not - not: phase=1,
% condensed: phase=2
phase=1;
% phase 1 : The temperature of the mass flow rate is constant --> constant
% temperature of the walls and of the heat flux through it; computed here
% once and for all
condens_resistance.R_o=0;
```

```
condens_resistance.R_m=0;
condens_resistance.R_fconv=0;

% External : radiation and natural convection
[condens_resistance]=Condens_heat_flux_external(CondensTank,Condens,phase,...
    condens_resistance);
% Conduction
[condens_resistance]=Condens_heat_flux_conduction(Condens,Material_condens,...
    condens_resistance);
% Internal : Forced convection
[condens_resistance]=Condens_heat_flux_internal(Condens,Extract,...
    Water,phase,condens_resistance);

condens_resistance.total=condens_resistance.R_o+condens_resistance.R_fconv...
    +condens_resistance.R_m;

%Iteration to ensure equal heat flux
q_fc=(Extract.T-Condens.T_m)/condens_resistance.R_fconv;
q_m=(Condens.T_m-Condens.T_ext)/condens_resistance.R_m;
q_o=(Condens.T_ext-CondensTank.T)/condens_resistance.R_o;

q_rel1=abs(q_fc - q_m);
q_rel2=abs(q_o - q_m);
q_rel=max(q_rel1,q_rel2);

Condens.T_m=Extract.T-(Extract.T-CondensTank.T)*condens_resistance.R_fconv...
    /condens_resistance.total;

Condens.T_ext=Condens.T_m-(Extract.T-CondensTank.T)*condens_resistance.R_m...
    /condens_resistance.total;

while(q_rel≥0.01)
    [condens_resistance]=Condens_heat_flux_conduction(Condens,...
        Material_condens,condens_resistance);
    [condens_resistance]=Condens_heat_flux_internal(Condens,Extract,...
        Water,phase,condens_resistance);
    [condens_resistance]=Condens_heat_flux_external(CondensTank,Condens,...
        phase,condens_resistance);
    condens_resistance.total=condens_resistance.R_o...
        +condens_resistance.R_fconv+condens_resistance.R_m;
    q_fc=(Extract.T-Condens.T_m)/condens_resistance.R_fconv;
    q_m=(Condens.T_m-Condens.T_ext)/condens_resistance.R_m;
    q_o=(Condens.T_ext-CondensTank.T)/condens_resistance.R_o;
    q_rel1=abs(q_fc - q_m);
    q_rel2=abs(q_o - q_m);
    q_rel=max(q_rel1,q_rel2);
    Condens.T_m=Extract.T-(Extract.T-CondensTank.T)...
        *condens_resistance.R_fconv/condens_resistance.total;
    Condens.T_ext=Condens.T_m-(Extract.T-CondensTank.T)...
        *condens_resistance.R_m/condens_resistance.total;
end
Grashof=9.81*Water.beta*(2*Condens.radius)^3*(Extract.T-Condens.T_m)...
    /Water.nu_vap^2;
Condens.Ri=Grashof/Condens.Reynolds^2;

Condens.L_condens=Condens.toCondens/(Extract.T-CondensTank.T)...
    *condens_resistance.total/(2*pi*Condens.radius);

% Cooling phase
phase=2;
```

```
length=0;
condens_losses=0;

[condens_resistance]=Condens_heat_flux_external(CondensTank,Condens,...
    phase,condens_resistance);
[condens_resistance]=Condens_heat_flux_conduction(Condens,...
    Material_condens,condens_resistance);
[condens_resistance]=Condens_heat_flux_internal(Condens,Extract,...
    Water,phase,condens_resistance);

Condens.Reynolds_cool=Condens.superficial_speed*Water.rho_vap/...
    Water.rho_liq*2*Condens.radius/Water.nu_liq;


while Extract.T>(60+273.15)
    condens_resistance.total=condens_resistance.total...
        /(2*pi*Condens.radius*Condens.ΔL);
    condens_losses=(Extract.T-CondensTank.T)/condens_resistance.total;
    T_out=Extract.T-condens_losses/Tank.flowrate_out/Water.C_p;
    Extract.T=T_out;
    Condens.T_m=Extract.T-1;
    Condens.T_ext=Extract.T-2;
    length=length+Condens.ΔL;
    q_rel=10;
    while(q_rel≥0.01)
        [condens_resistance]=Condens_heat_flux_external(CondensTank,...
            Condens,phase,condens_resistance);
        [condens_resistance]=Condens_heat_flux_conduction(Condens,...
            Material_condens,condens_resistance);
        [condens_resistance]=Condens_heat_flux_internal(Condens,...
            Extract,Water,phase,condens_resistance);
        condens_resistance.total=condens_resistance.R_o...
            +condens_resistance.R_fconv+condens_resistance.R_m;
        q_fc=(Extract.T-Condens.T_m)/condens_resistance.R_fconv;
        q_m=(Condens.T_m-Condens.T_ext)/condens_resistance.R_m;
        q_o=(Condens.T_ext-CondensTank.T)/condens_resistance.R_o;
        q_rel1=abs(q_fc - q_m);
        q_rel2=abs(q_o - q_m);
        q_rel=max(q_rel1,q_rel2);
        Condens.T_m=Extract.T-(Extract.T-CondensTank.T)...
            *condens_resistance.R_fconv/condens_resistance.total;
        Condens.T_ext=Condens.T_m-(Extract.T-CondensTank.T)...
            *condens_resistance.R_m/condens_resistance.total;
    end
    condens_resistance.total=condens_resistance.R_o...
        +condens_resistance.R_fconv+condens_resistance.R_m;
end
Grashof_cool=9.81*Water.beta*(2*Condens.radius)^3*...
    (Extract.T-Condens.T_m)/Water.nu_liq^2;
Prandtl_cool=Water.mu_liq*Water.C_p/Water.thermal_cond_liq;
Raleigh_cool=Grashof_cool*Prandtl_cool;
Condens.Ri_cool=Grashof_cool/Condens.Reynolds_cool^2;
Condens.cooling_length=length;
Condens.total_length=Condens.cooling_length+Condens.L_condens;
```

Functions

```
function [h] = Parabola_losses(T_p,Site,Parabola,Air,mirror)

% Heat losses
```

```

%% Radiation
sigma=5.6703e-8; %Stefan-Boltzmann constant
if mirror==1
    eps=0.9; % Glass.
else
    eps=0.09;
end
h.rad=sigma*eps*(Site.T_sky^2+T_p^2)*(Site.T_sky+T_p);
%% Natural convection

Grashof=9.81*Air.beta*Parabola.L^3*(T_p-Site.T_atm)/Air.nu^2;
Prandtl=Air.mu*Air.C_p/Air.thermal_cond;
Raleigh=Grashof*Prandtl;
Nusselt=0.54*Raleigh^(1/4);
h.conv=Nusselt*Air.thermal_cond/Parabola.L;
h.tot=h.rad+h.conv; %per unit of inner surface
```

```
function [resistance]=Condens_heat_flux_internal(Condens,Extract,...
    Water,phase,resistance)

%% Simple pipe

% isotherm wall

% Phase 1 : vapor
if phase==1
Re=Condens.superficial_speed*2*Condens.radius/Water.nu_vap;
% International Steam Tables: Properties of Water and Steam on GoogleBooks
Pr=1.7518;
if Re<2300
    Nusselt_T=4.36;
elseif Re<4000
frict=(1.82*log10(Re)-1.64)^(-2);
Nusselt_T=(frict/8)*(Re-1000)*Pr/(1+12.7*(frict/8)^0.5*(Pr^(2/3)-1));
else
Nusselt_T=0.023*Re^0.8*Pr^0.4;
end
h_fconv=Nusselt_T*Water.thermal_cond_vap/(2*Condens.radius);

% Phase 2 : liquid
elseif phase==2
Re=Condens.superficial_speed*2*Condens.radius/Water.nu_liq;

Gr=9.81*Water.beta*(2*Condens.radius)^3*(Extract.T-Condens.T_m)...
    /Water.nu_liq^2;
Pr=Water.mu_liq*Water.C_p/Water.thermal_cond_liq;
Ra=Gr*Pr;
Nusselt_T=3.18935*(Ra/Re)^0.26352;
h_fconv=Nusselt_T*Water.thermal_cond_liq/(2*Condens.radius);
end

resistance.R_fconv=1/h_fconv;
```

```
function [resistance] = Condens_heat_flux_conduction(Condens,...
    Material_condens,resistance)

```

```
%% metal

resistance.R_m=log((Condens.radius+Condens.thickness)/Condens.radius)...
    /Material_condens.cond*(Condens.radius); %per unit inner surface
```

```
function [resistance] = Condens_heat_flux_external(CondensTank,Condens...
    ,phase,resistance)

%% Radiation

sigma=5.6703e-8; %Stefan-Boltzmann constant
eps=0.85; % Stainless steel weathered.
h_rad=sigma*(CondensTank.T^2+Condens.T_ext^2)...
    *(CondensTank.T+Condens.T_ext)/(1/eps+0.1*(1-eps)/eps);

%% Natural convection
water.beta= 2.14e-4; %[/K] engineering toolbox
water.density=992.22; %[kg/m^3] engineering toolbox
water.C_p=4180; %[kg/m^3/K] engineering toolbox at 40degC
water.nu=0.553e-6; %[m^2/s] engineering toolbox at 50degC
water.thermal_cond=0.58; %[W/m/K] engineering toolbox
water.mu=water.nu*water.density;
Grashof=9.81*water.beta*(2*Condens.radius+2*Condens.thickness)^3*...
    (Condens.T_ext-CondensTank.T)/water.nu^2;
Prandtl=water.mu*water.C_p/water.thermal_cond;
Raleigh=Grashof*Prandtl;

if Raleigh≤1e-2
    C=0.675;
    n=0.058;
elseif Raleigh≤1e2
    C=1;
    n=0.148;
elseif Raleigh≤1e4
    C=0.85;
    n=0.188;
elseif Raleigh≤1e7
    C=0.48;
    n=0.25;
elseif Raleigh≤1e12
    C=0.125;
    n=0.333;
end

Nusselt=C*Raleigh^n;
h_conv=Nusselt*water.thermal_cond/(2*Condens.radius+2*Condens.thickness);

resistance.R_o=1/(h_rad+h_conv)*(Condens.radius)...
    /(Condens.radius+Condens.thickness); %per unit of inner surface
```

Appendix C

Arc Length of the Parabola

A parabola of focal distance p is characterised by the following equation:

$$f(x) = \frac{x^2}{4p}$$

If the focal distance is fixed to 0.5 m, the equation becomes: $f(x) = \frac{x^2}{2}$.
The arc length of a parabola comprised between its focal axis and a given value x_e of the X axis is given by:

$$L = \int_0^{x_e} \sqrt{1 + f'(x)^2}\mathrm{dx}$$

which gives the following integral to solve:

$$L = \int_0^{x_e} \sqrt{1 + x^2}\mathrm{dx}$$

This can be done by setting $x = \mathrm{sh}u$, which gives

$$\int_0^{u_e} \sqrt{\mathrm{ch}^2 u}\,\mathrm{ch}u\mathrm{du}$$

with $u_e = \mathrm{arcsh}x_e$.
Knowing that $chu = \frac{[\exp u + \exp(-u)]}{2}$, the solution of the integral is

$$L = \frac{1}{2}u_e + \frac{1}{8}\left[\exp 2u_e + \exp(-2u_e)\right]$$

The latest equation can be solved for u_e considering for L the wanted half length of parabolic arc, here 0.5 m.
The corresponding value of x_e can then easily be recovered. The result obtained is $x_e = 48$cm, which corresponds to a total width of parabola of 96 cm.